

Computer-Aided Diagnosis of Breast Cancer: Towards the Detection of Early and Subtle Signs



SCHULICH
School of Engineering



Rangaraj M. Rangayyan
J. E. Leo Desautels
Fábio José Ayres



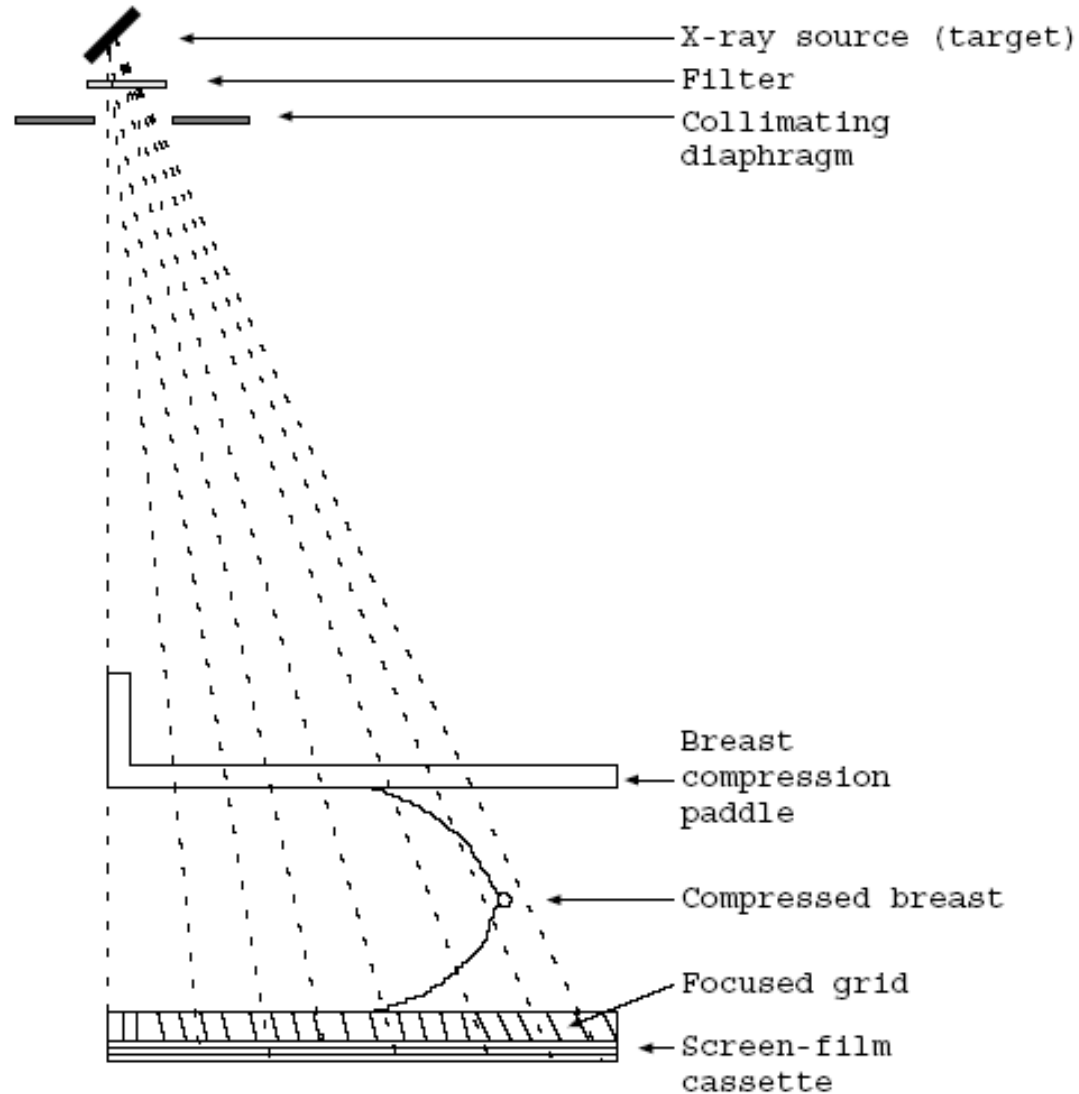
Department of Electrical and Computer
Engineering, University of Calgary
Alberta Cancer Board: Screen Test
Calgary, Alberta, CANADA



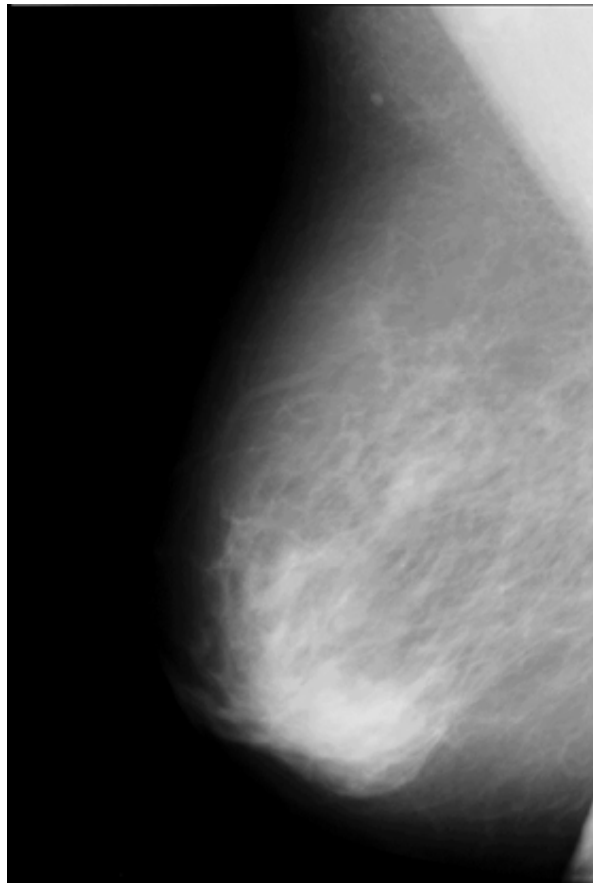
Breast cancer statistics

- Lifetime probability of developing breast cancer is one in 8.8 (Canada)
- Lifetime probability of death due to breast cancer is one in 27 (Canada)
- Prevalence: 1% of all women living with the disease
- Screening mammography has been shown to reduce mortality rates by 30% to 70%

X-ray imaging of the breast



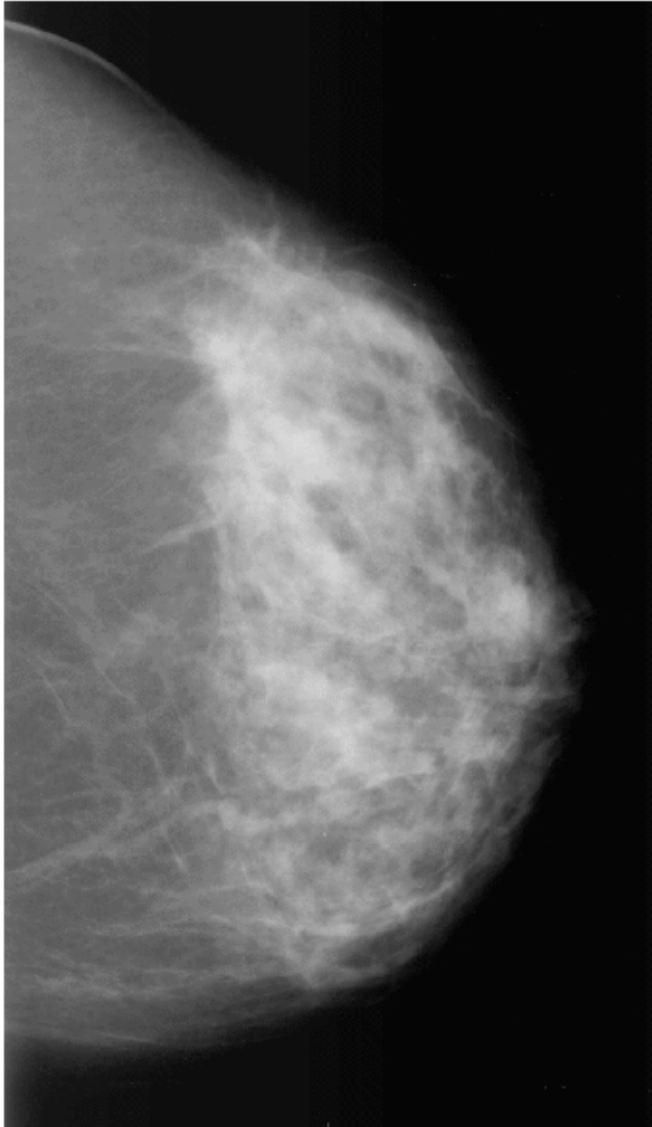
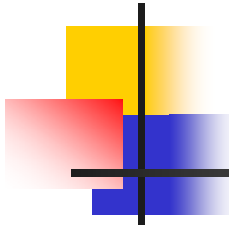
Mammography



Signs of Breast Cancer:

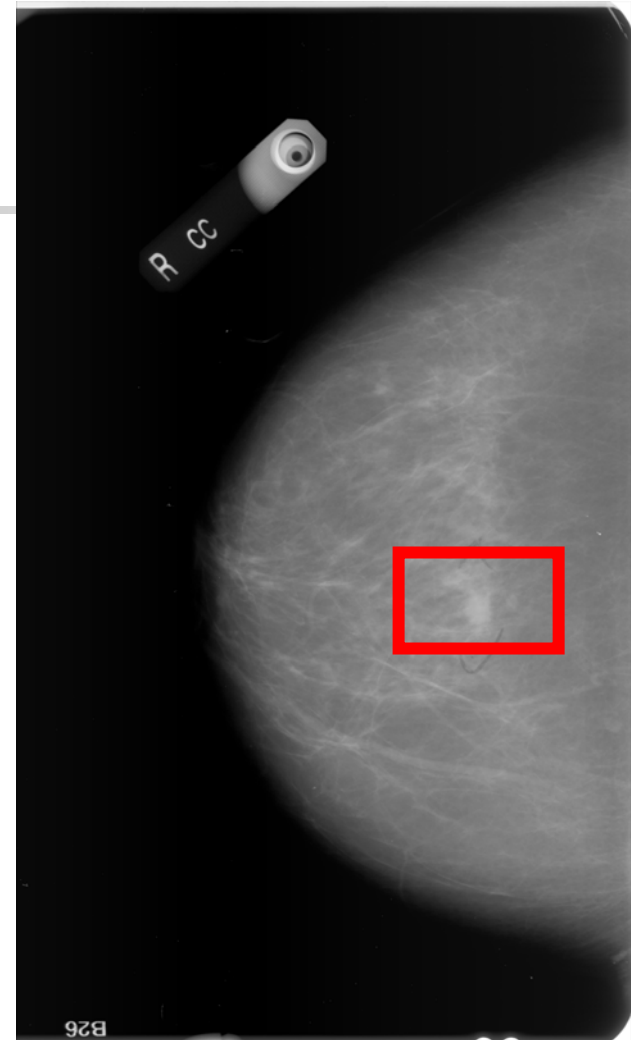
- Masses
- Calcifications
- Bilateral asymmetry
- Architectural distortion (subtle, often missed)

Two standard views per breast: Cranio-caudal and Mediolateral oblique



Masses

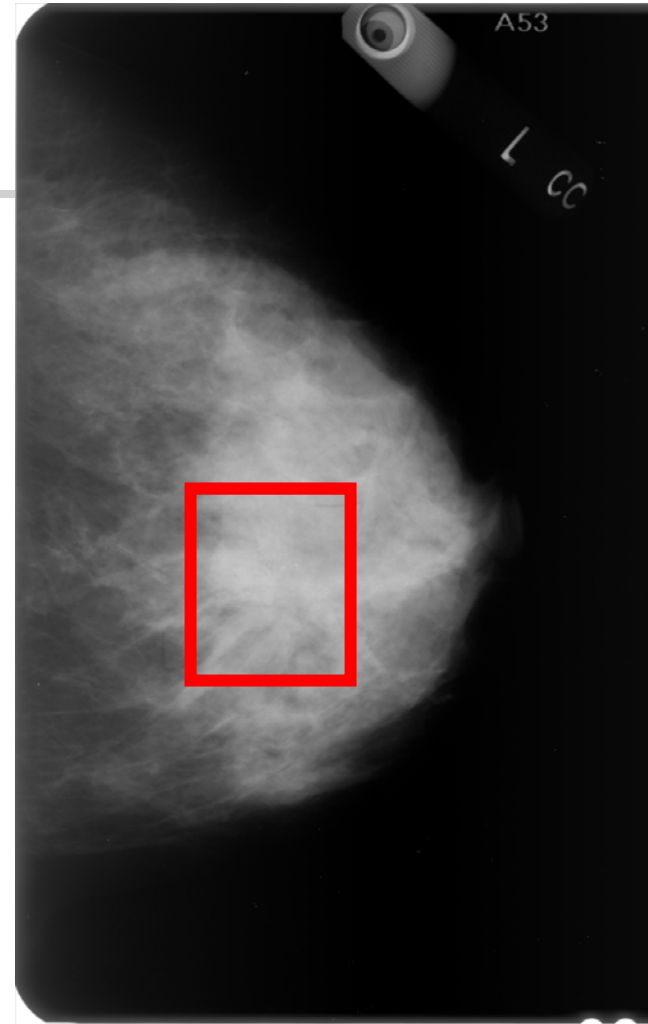
- Breast cancer causes a desmoplastic reaction in breast tissue
- A mass is observed as a bright, hyper-dense object



Mammogram with a mass

Calcification

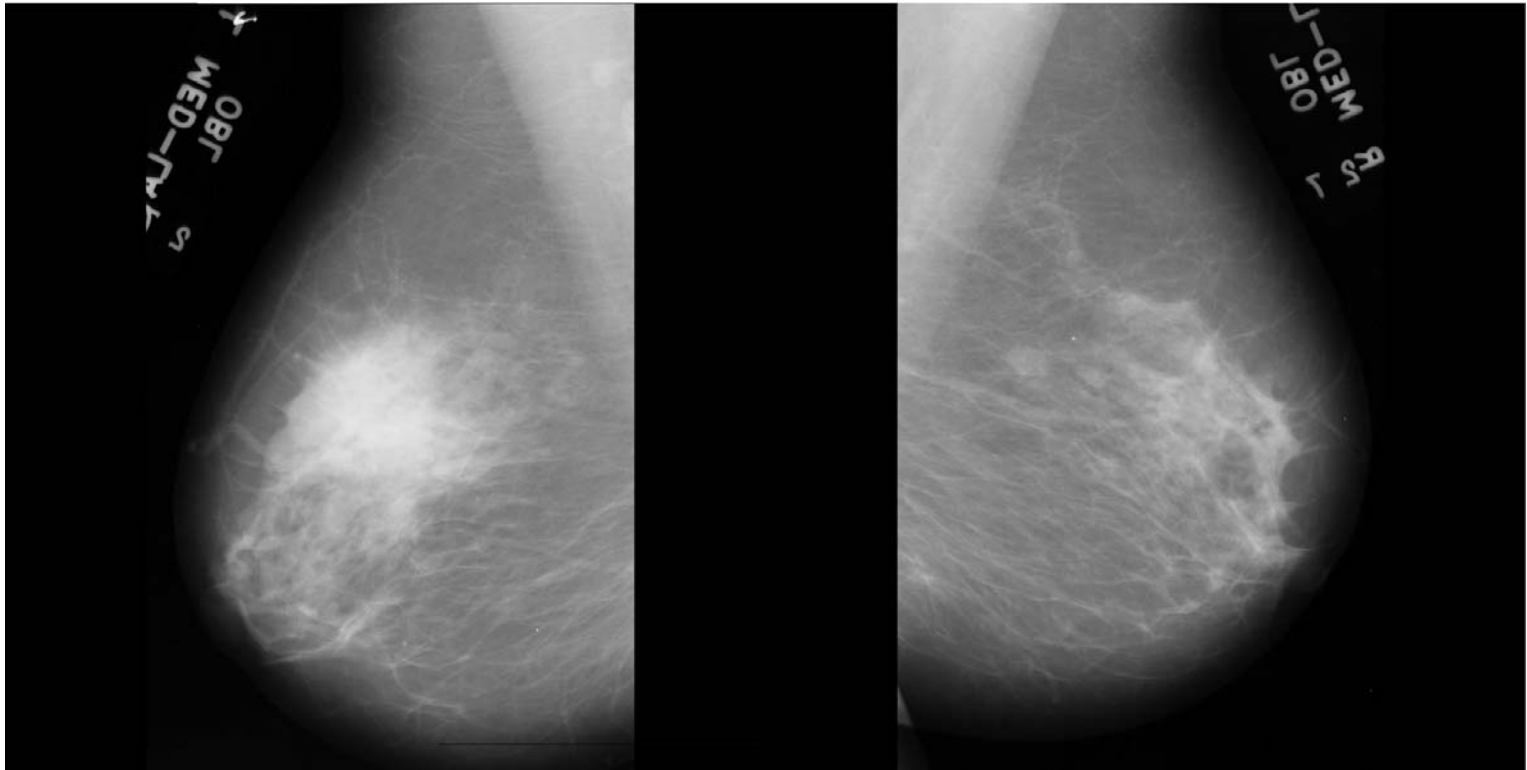
- Deposits of calcium in breast tissue



Mammogram with calcification

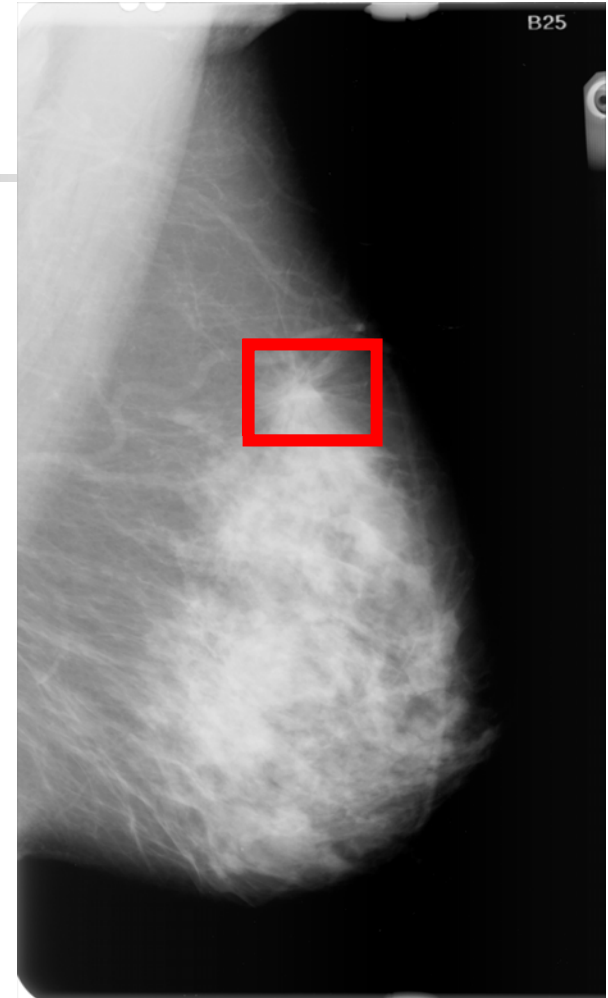
Bilateral Asymmetry

- Differences in the overall appearance of one breast with reference to the other



Architectural Distortion

- Third most common mammographic sign of nonpalpable breast cancer
- The normal architecture of the breast is distorted
- No definite mass visible
- Spiculations radiating from a point
- Focal retraction or distortion at the edge of the parenchyma



Mammogram with architectural distortion



Objectives of computer-aided processing of mammograms

- Enhancement of image quality
- Detection of subtle signs of cancer
- Quantitative analysis of features
- Objective aids to diagnostic decision
- Accurate and consistent analysis
- ***Earlier detection of breast cancer!***



Some important problems

Detection of:

- Breast boundary (skin – air boundary)
- Pectoral muscle (in MLO views)
- Fibro-glandular disc
- Calcifications
- Masses and tumors
- Curvilinear structures
- Bilateral asymmetry (asymmetric densities)
- Architectural distortion



Computer-aided diagnosis (CAD)

- Increased number of cancers detected¹ by 19.5%
- Increased early-stage malignancies detected¹ from 73% to 78%
- Recall rate increased¹ from 6.5% to 7.7%
- 50% of the cases of architectural distortion missed²

¹ (Freer and Ulisse, 2001) ² (Baker et al., 2003)



Simultaneous contrast





Simultaneous contrast

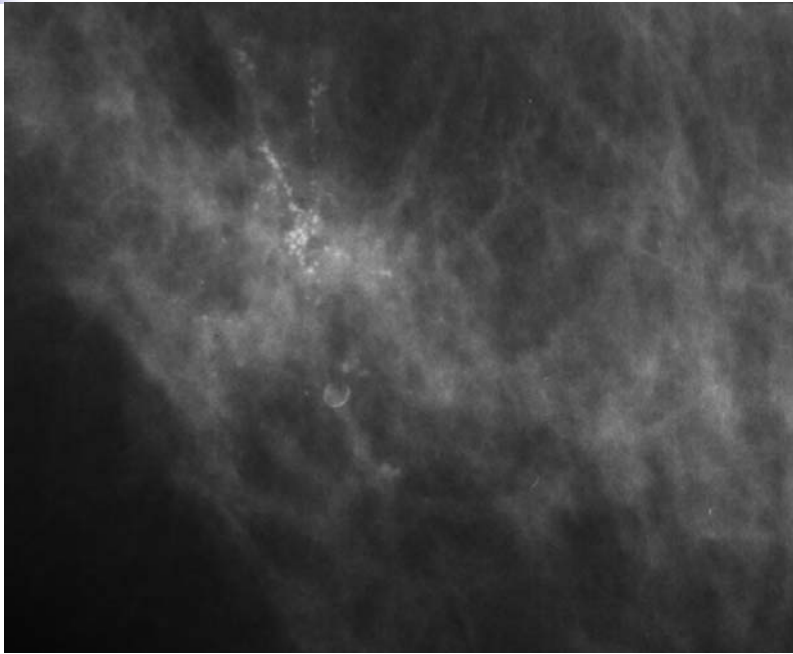




Just-noticeable difference



Contrast enhancement

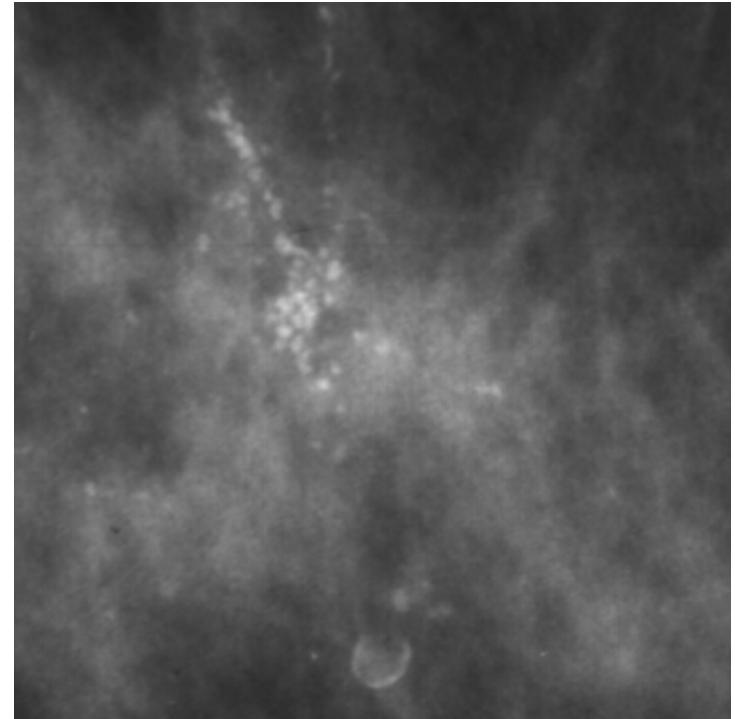
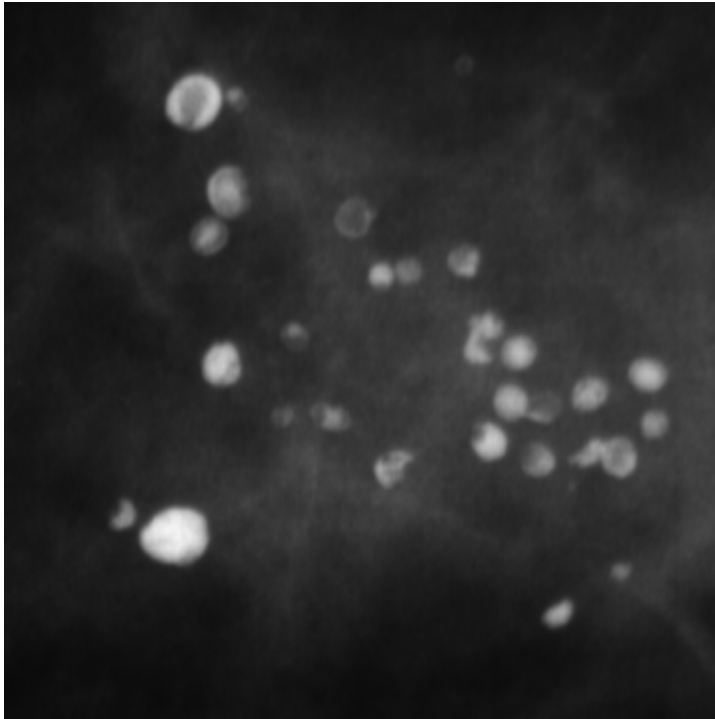


Original mammogram
with calcifications

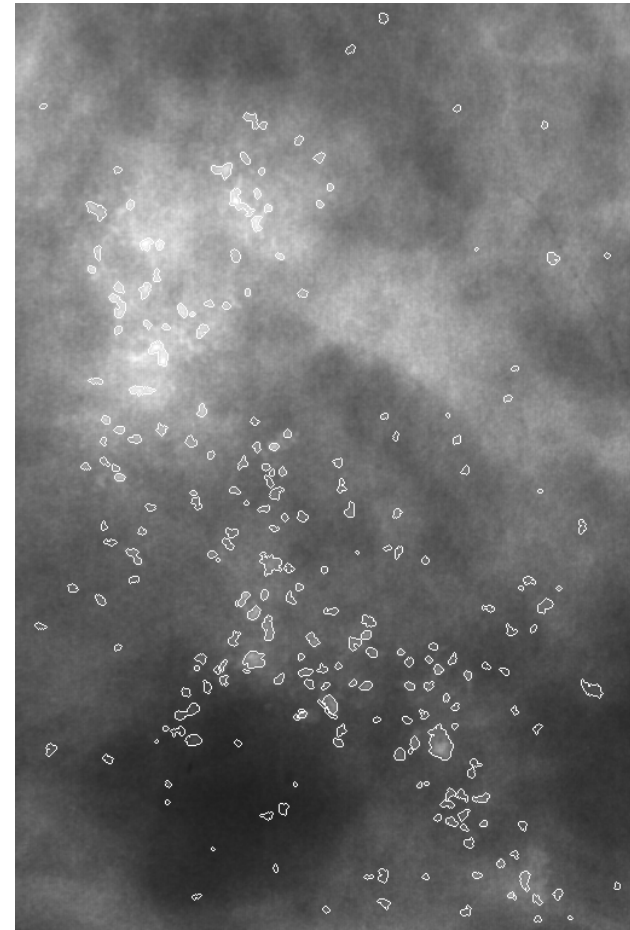
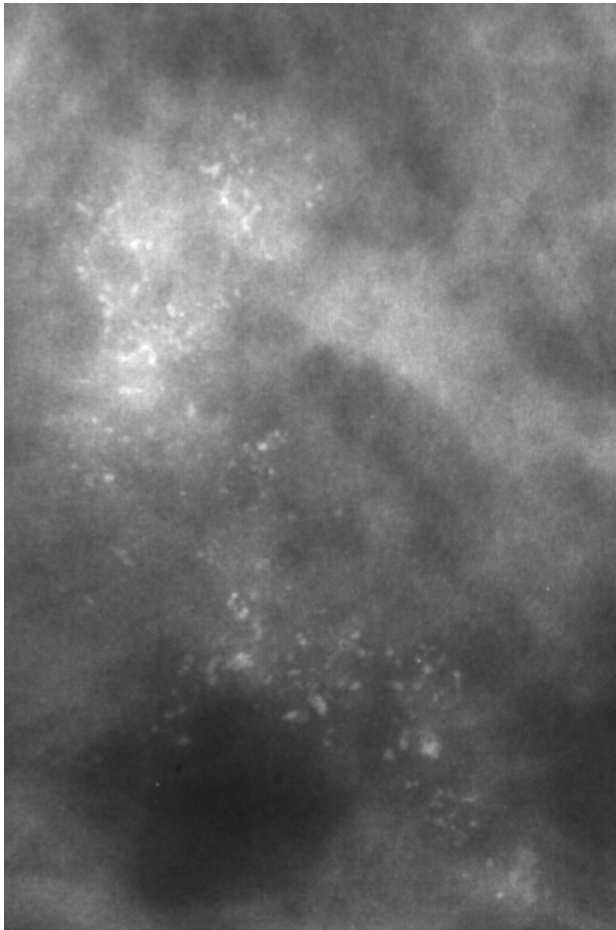


Enhanced image
using adaptive-neighborhood
contrast enhancement

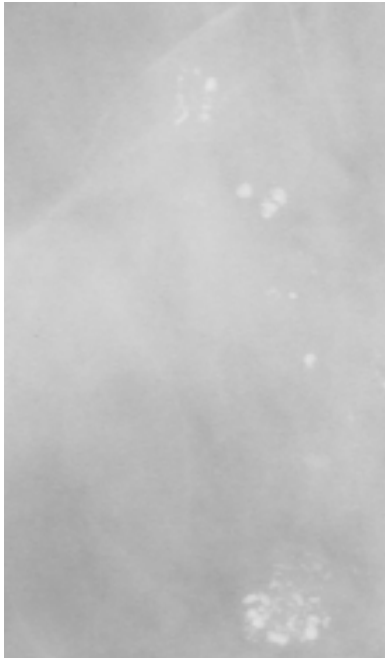
Examples of benign and malignant calcifications



Detection of calcifications by region growing



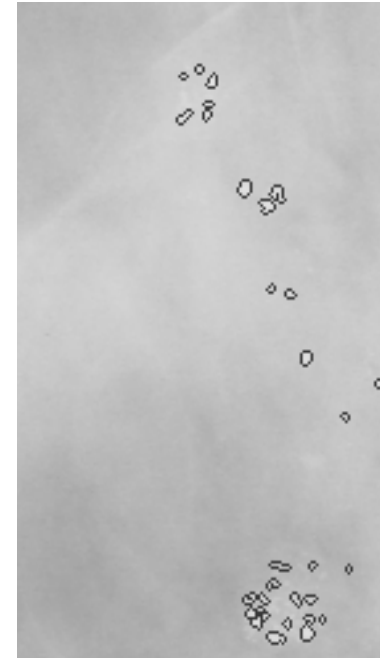
Detection of calcifications by error of prediction



(a) Part of original mammogram

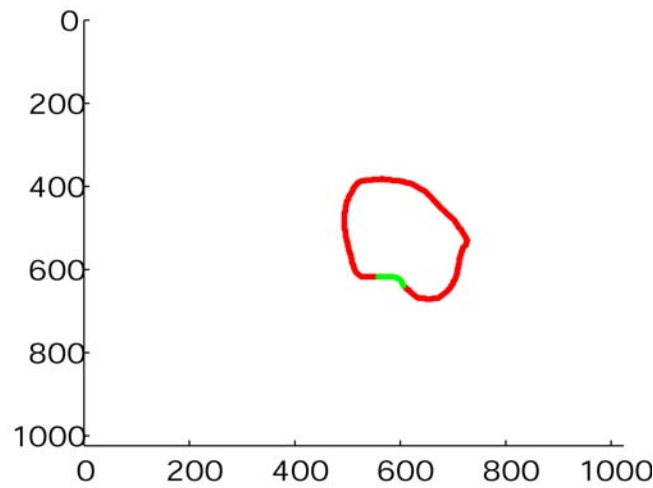
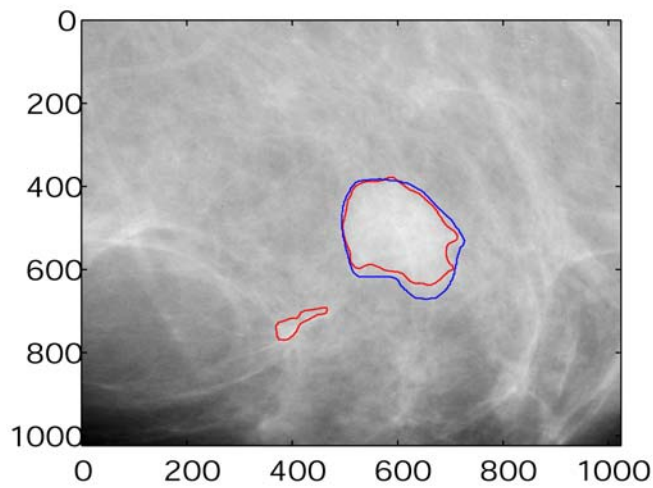
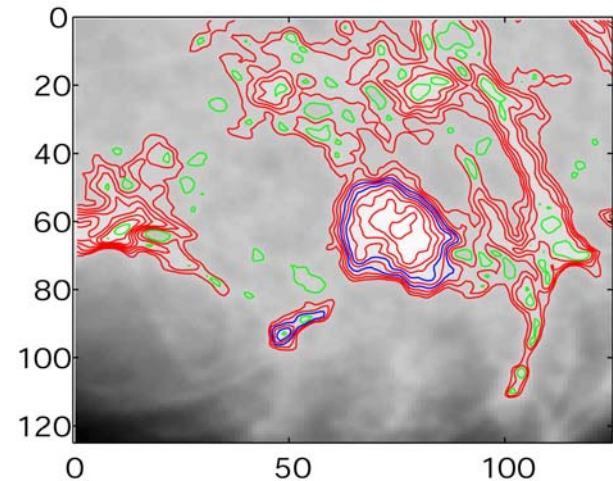
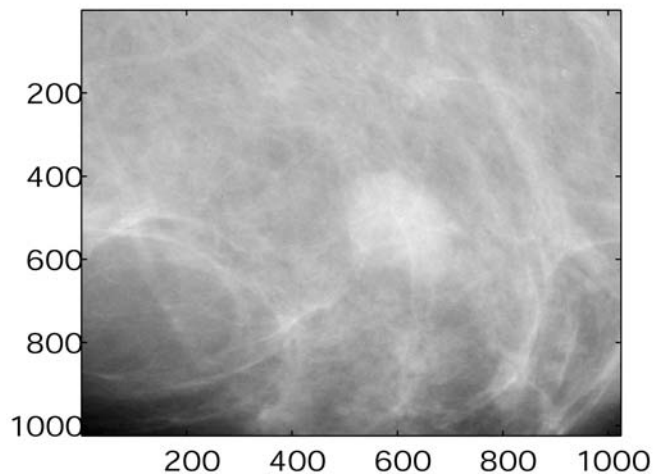
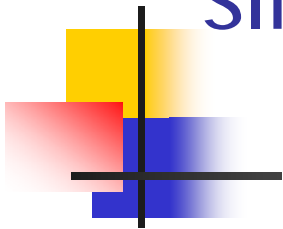


(b) Seeds detected using prediction error



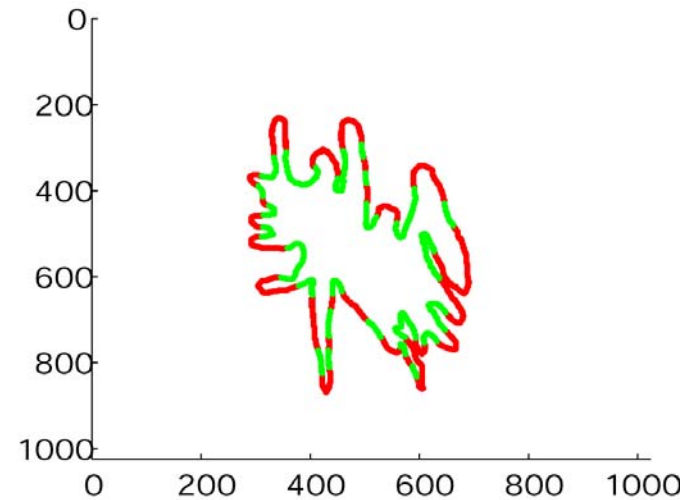
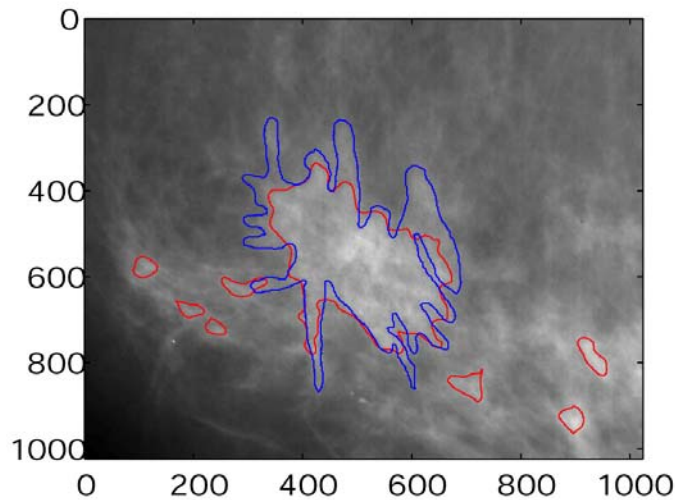
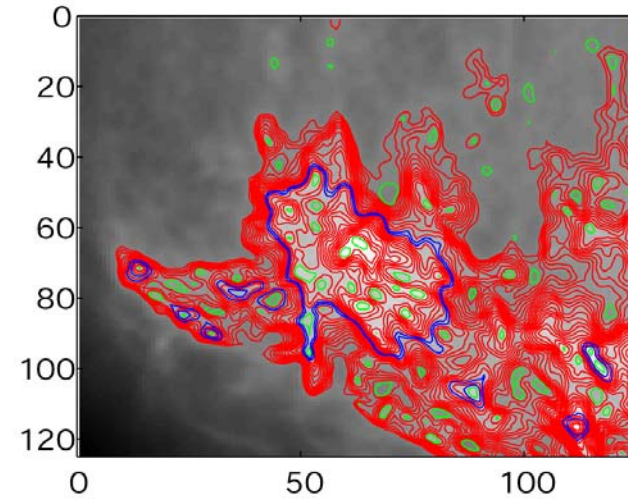
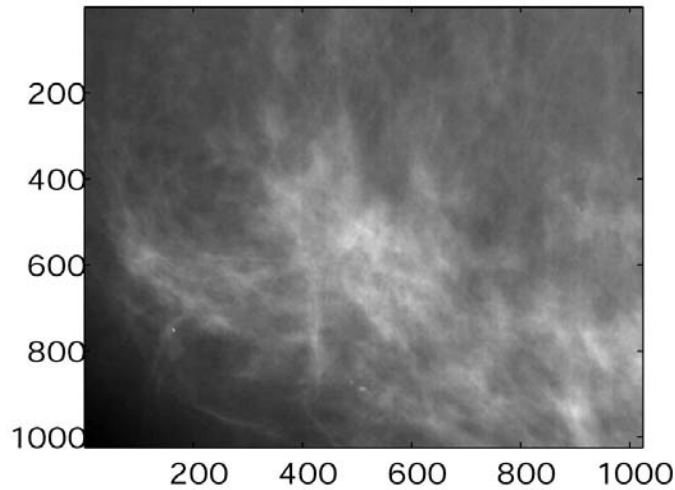
(c) Calcifications detected by region growing

Detection of masses by density slicing and texture flow-field analysis



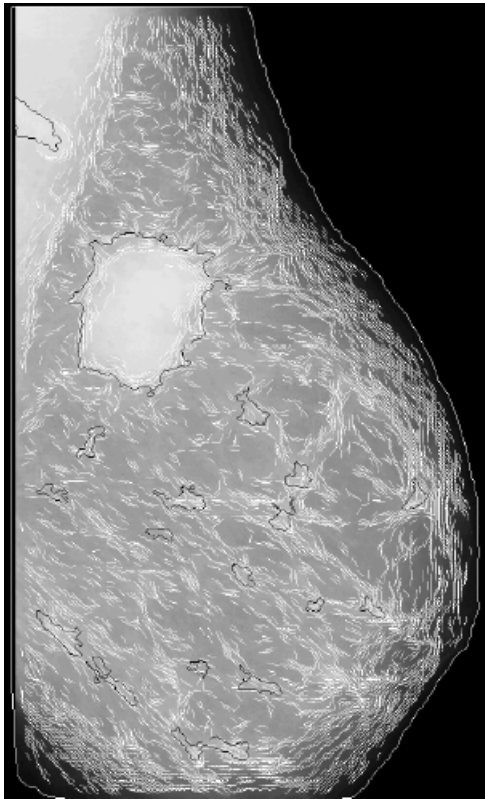
Most benign masses have smooth shapes with convex lobules.

Detection and analysis of tumors

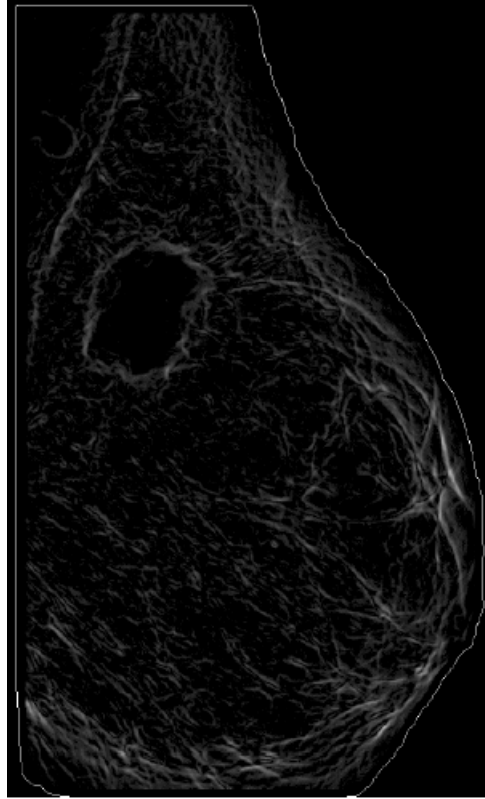


The green parts of the boundary represent concave segments, indicating malignancy.

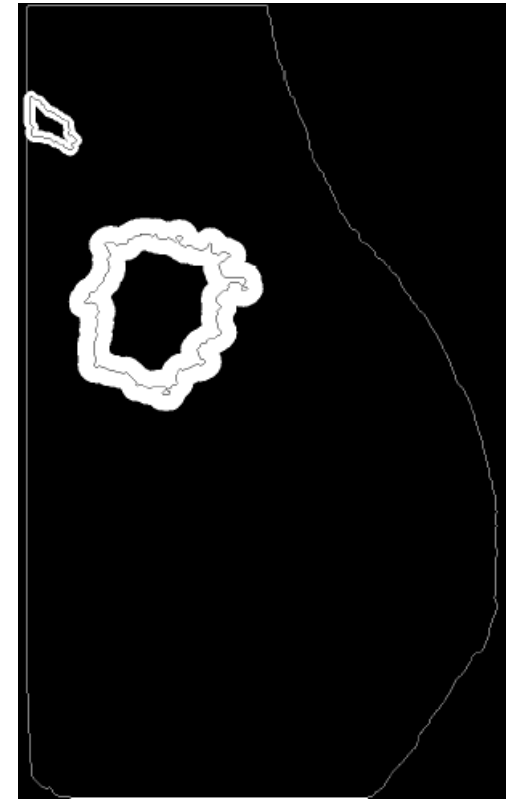
Detection and analysis of tumors



Orientation field

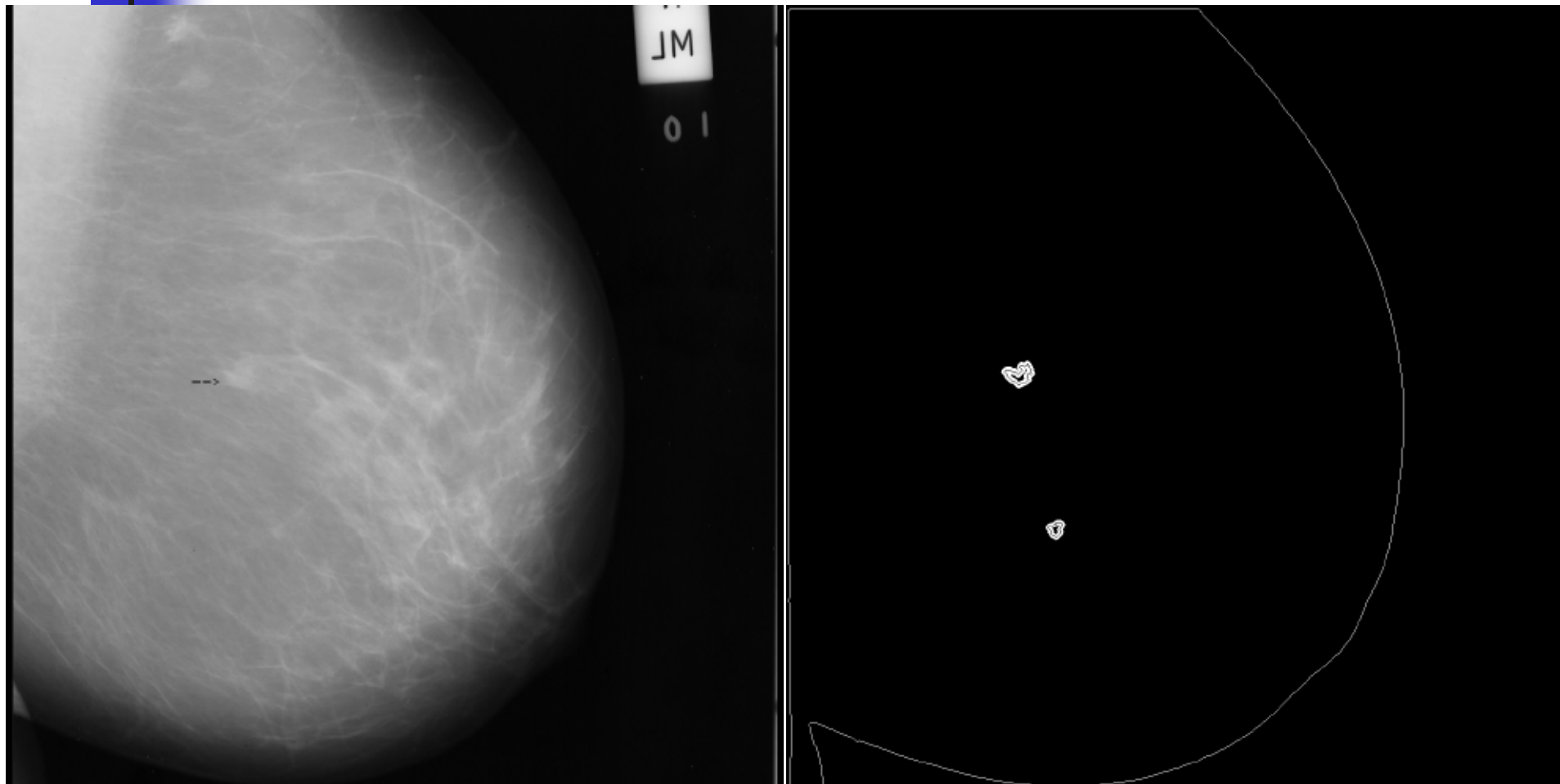


Coherence

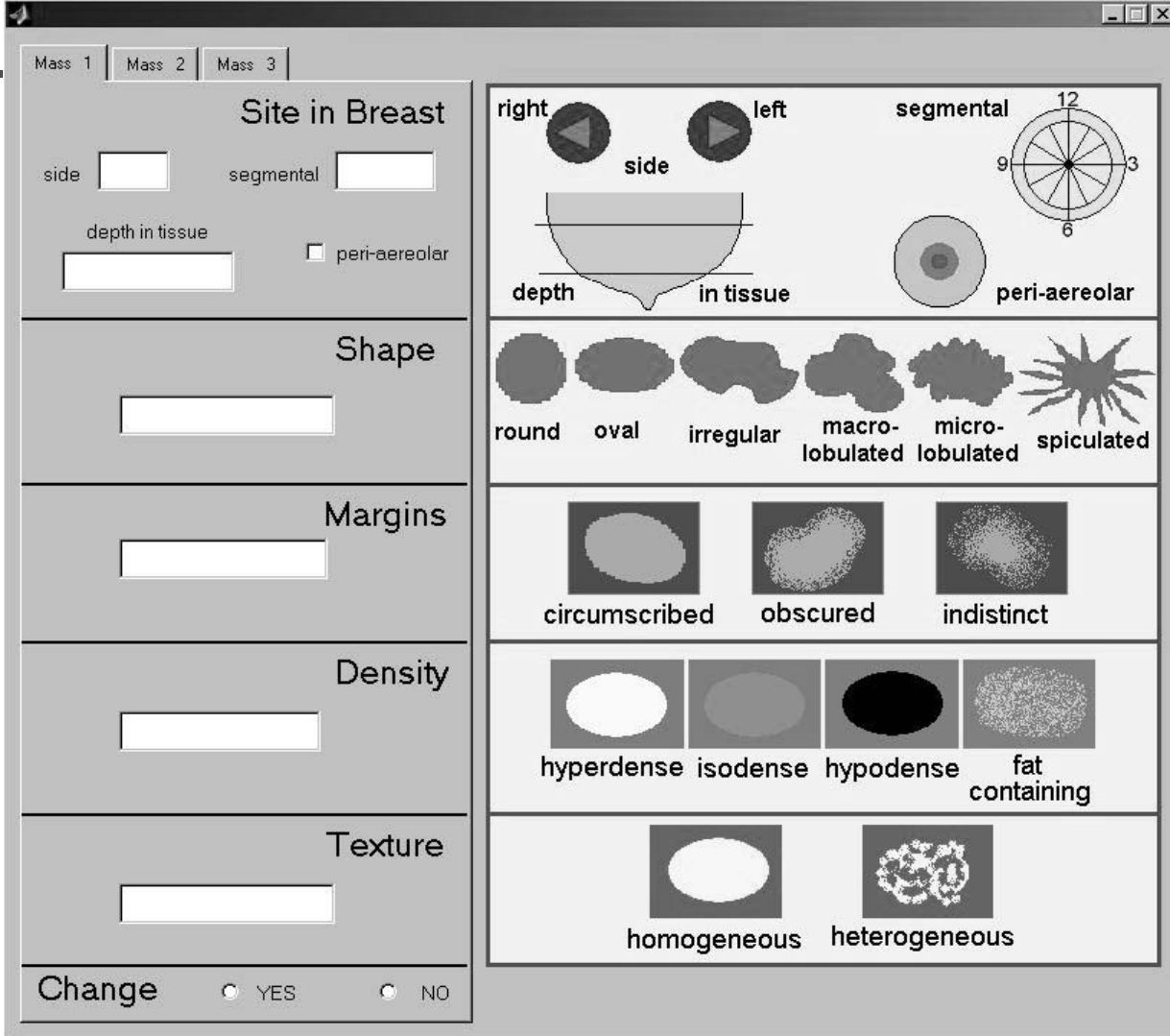


Tumor + FP detected

Detection of a subtle tumor



Radiological characterization of masses (BI-RADS)



Mass 1 Mass 2 Mass 3

Site in Breast

side segmental

depth in tissue peri-aereolar

Shape

Margins

Density

Texture

Change YES NO

right left side segmental

depth in tissue peri-aereolar

round oval irregular macro-lobulated micro-lobulated spiculated

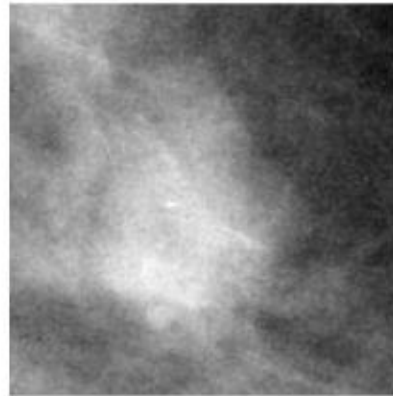
circumscribed obscured indistinct

hyperdense isodense hypodense fat containing

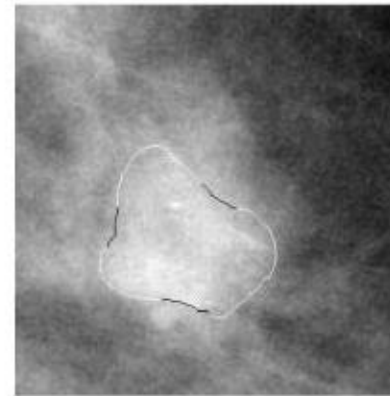
homogeneous heterogeneous

Analysis of masses: feature extraction

Mass region



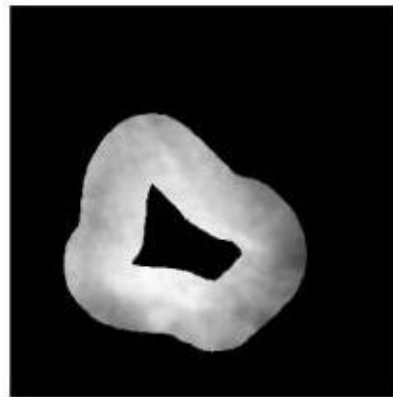
(a)



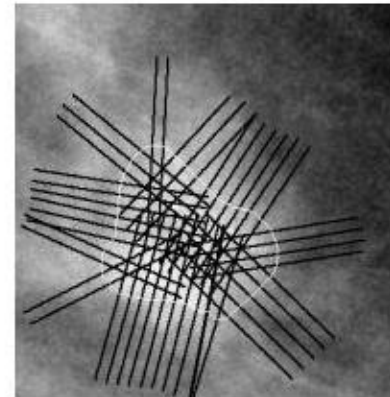
(b)

Shape analysis:
Fractional concavity

Ribbon for computation of texture features



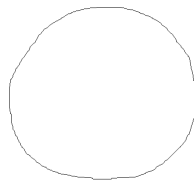
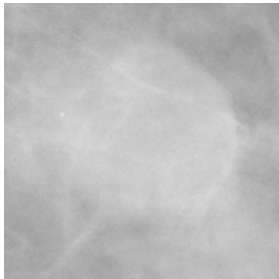
(c)



(d)

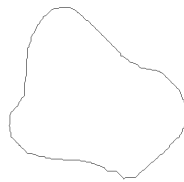
Normals to contour for computation of edge sharpness (acutance)

Objective representation of breast masses



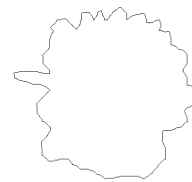
(a) b145lc95
 $F_{cc} = 0.00$
 $A = 0.07$
 $F_8 = 8.11$

**benign
circumscribed**



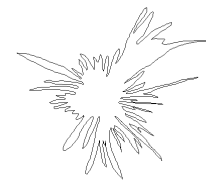
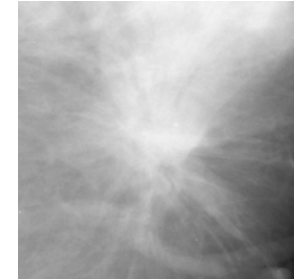
(b) b164ro94
 $F_{cc} = 0.42$
 $A = 0.08$
 $F_8 = 8.05$

**benign
macrolobulated**



(c) m51rc97
 $F_{cc} = 0.64$
 $A = 0.09$
 $F_8 = 8.15$

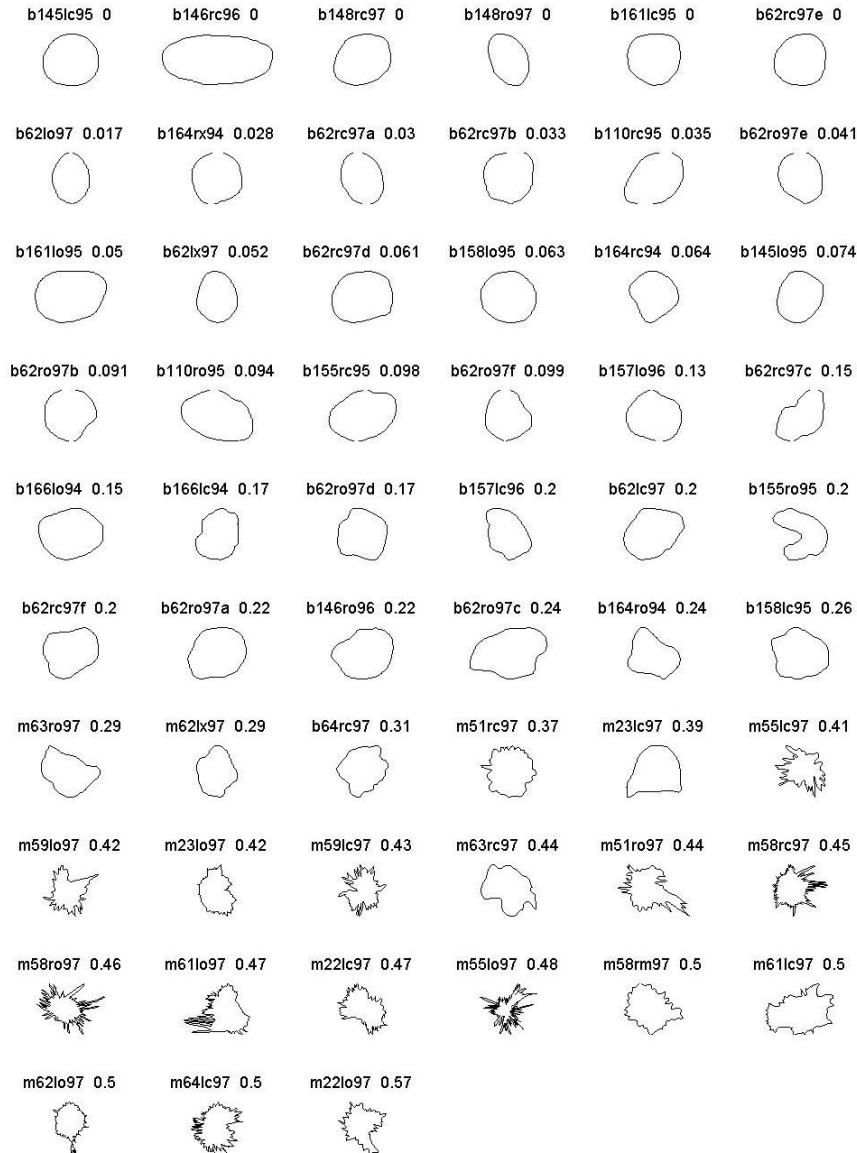
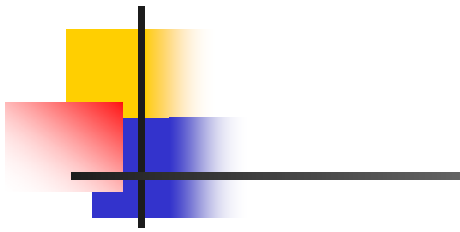
**malignant
microlobulated**



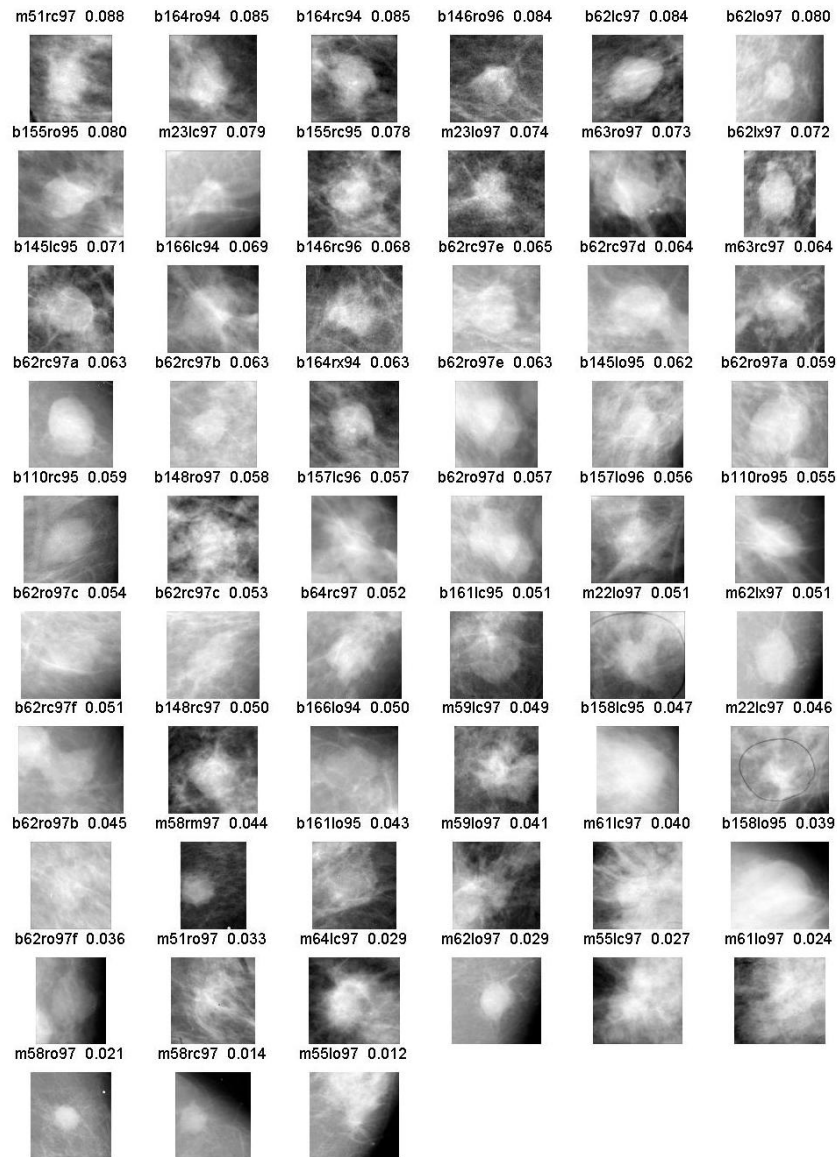
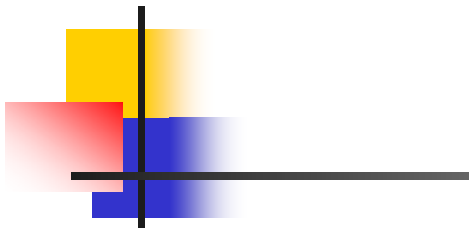
(d) m55lo97
 $F_{cc} = 0.83$
 $A = 0.01$
 $F_8 = 8.29$

**malignant
spiculated**

Rank-ordering using shape: F_{CC}



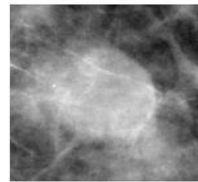
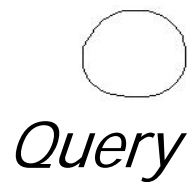
Rank-ordering using acutance



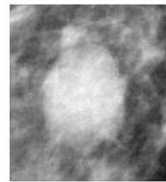
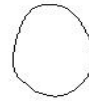
Classification of masses

	Logistic regression			Mahalanobis (pooled)			Linear discriminant analysis				KNN = 7			Recall
Features	Sens	Spec	Avg	Sens	Spec	Avg	Sens	Spec	Avg	A_z	Sens	Spec	Avg	Avg
F_{cc}	90	97.3	94.7	90	97.3	94.7	100	97.3	98.2	0.99	90	97.3	94.7	90.4
A	50	94.6	78.9	75	67.6	70.0	75.0	73.0	73.7	0.73	45	91.7	73.7	63.6
F_8	30	86.5	66.7	65	56.8	59.6	75.0	54.0	61.4	0.68	25	67.6	52.6	53.5
F_{cc}, A	90	97.3	94.7	90	97.3	94.7	100	97.3	98.2	0.98	90	100	96.5	84.6
F_{cc}, F_8	90	97.3	94.7	90	97.3	94.7	100	97.3	98.2	0.99	90	97.3	94.7	85.6
A, F_8	55	86.5	75.4	60	70.3	66.7	75.0	73.0	73.7	0.76	55	89.2	73.7	61.6
F_{cc}, A, F_8	90	97.3	94.7	95	97.3	96.5	100	97.3	98.2	0.99	90	97.3	94.7	83.4
14 texture	*	*	*	70	50.0	64.9	65.0	64.9	64.9	0.67	#	#	#	#

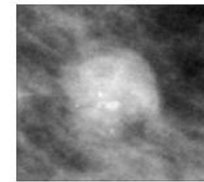
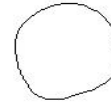
Content-based retrieval and analysis: benign mass



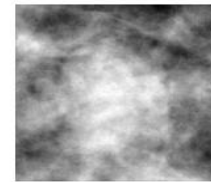
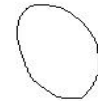
b145lc95



b62lx97

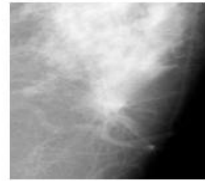
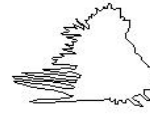


b164rx94

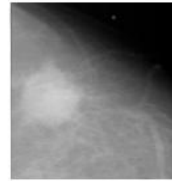


b148ro97

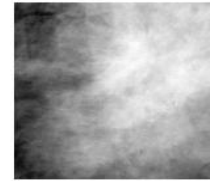
Content-based retrieval and analysis: malignant tumor



m55lo97



m58rc97

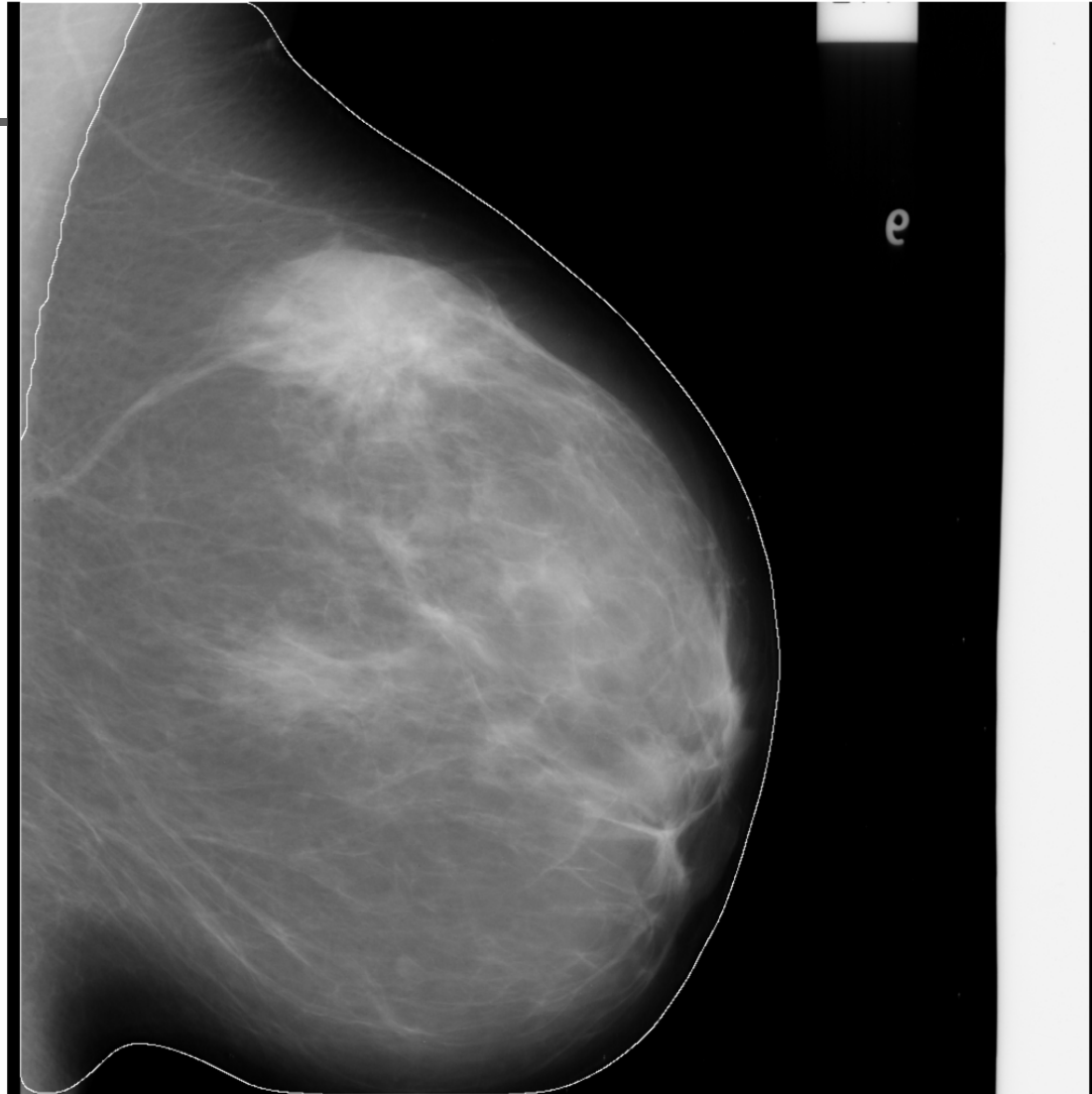
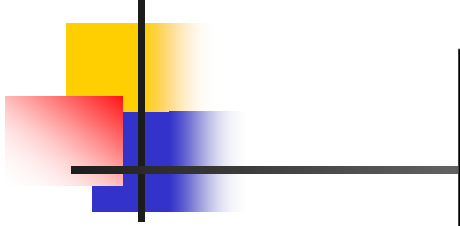


m61lo97

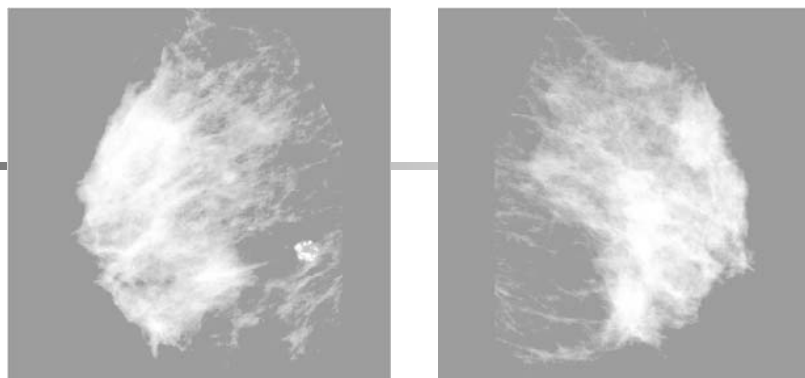
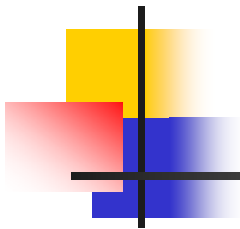


m55lc97

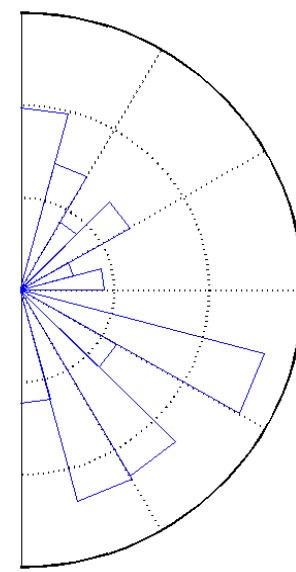
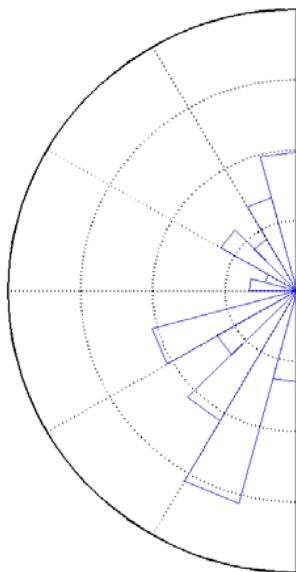
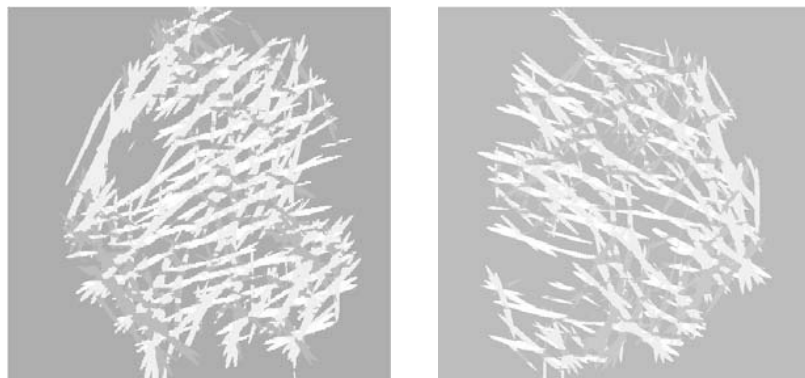
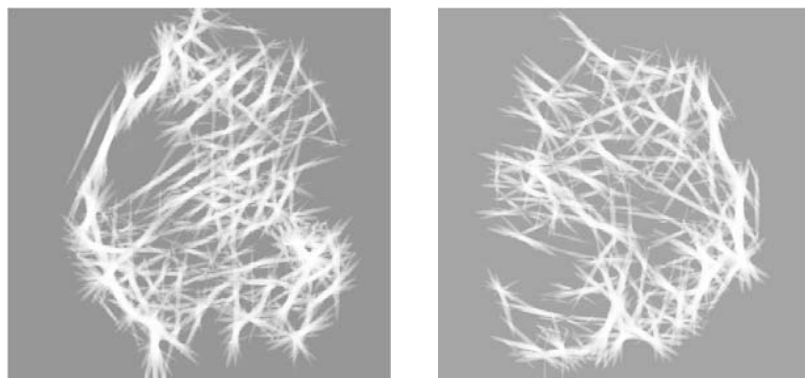
Detection of the pectoral muscle edge and the breast boundary using Gabor filters and active contour models



Analysis of bilateral asymmetry using Gabor filters

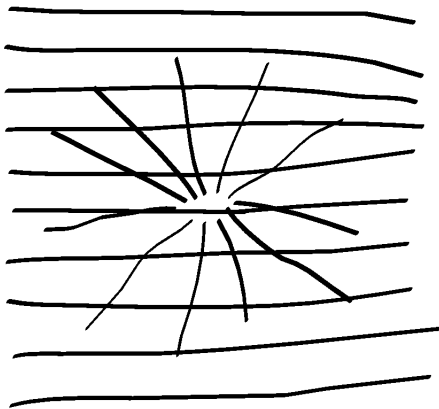


The directional distribution of fibroglandular tissue differs between the left and right breasts

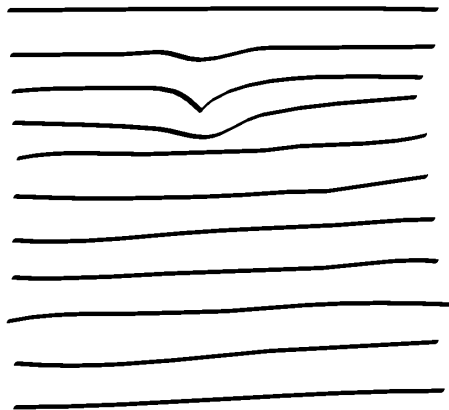




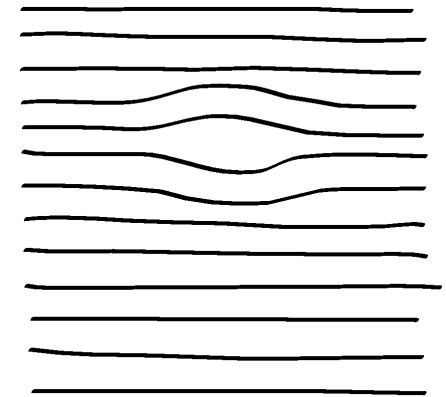
Architectural distortion



spiculated

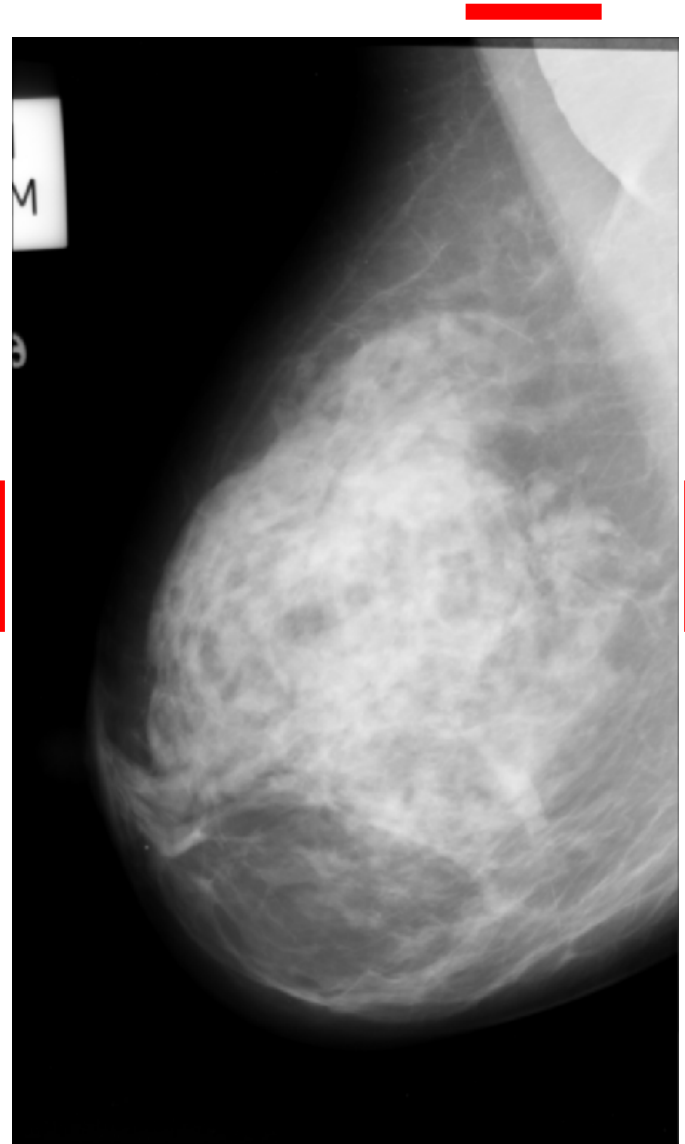
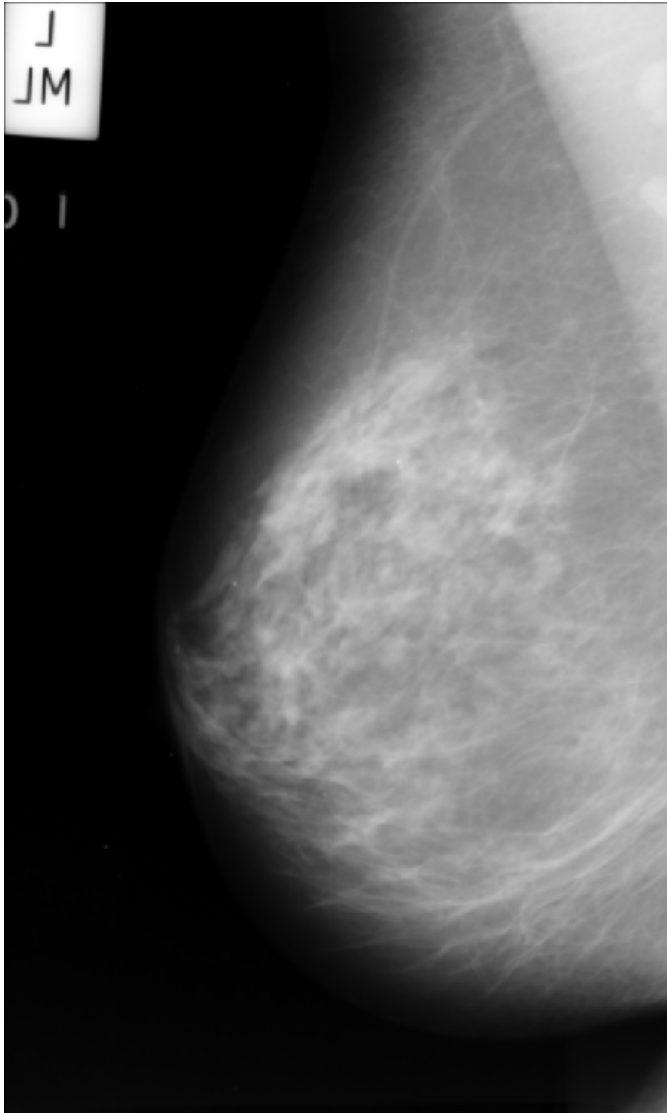


focal retraction

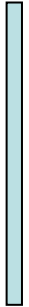
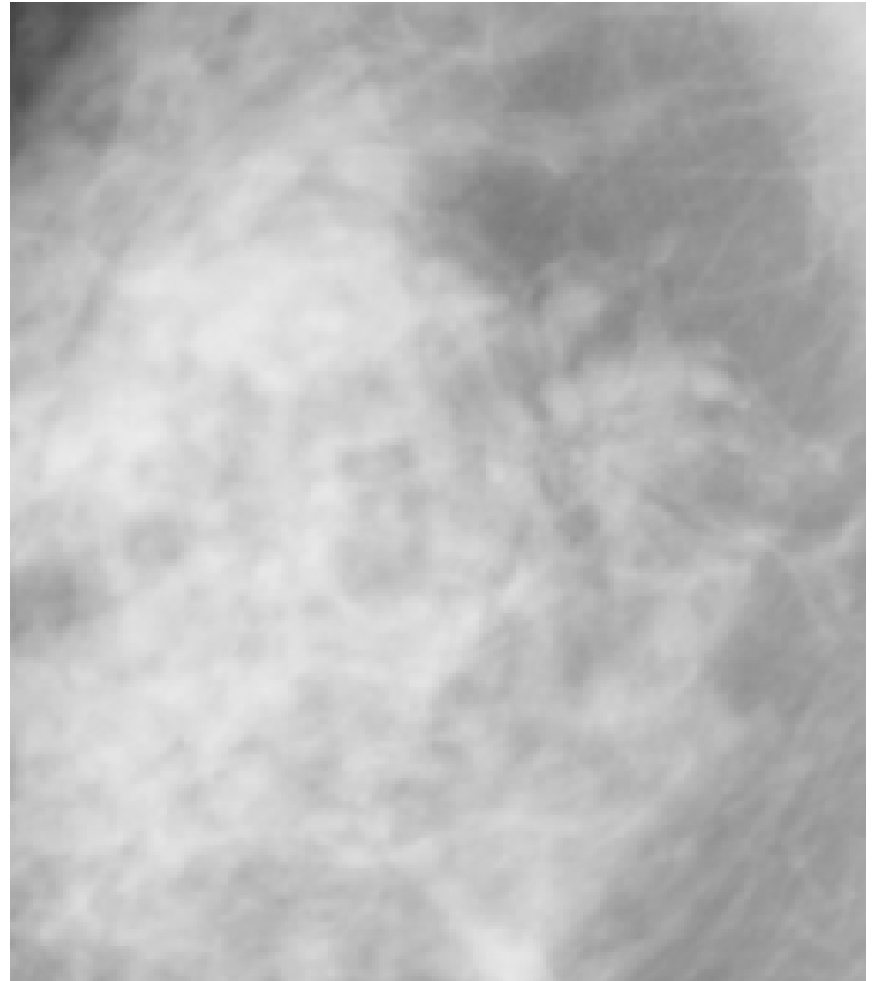
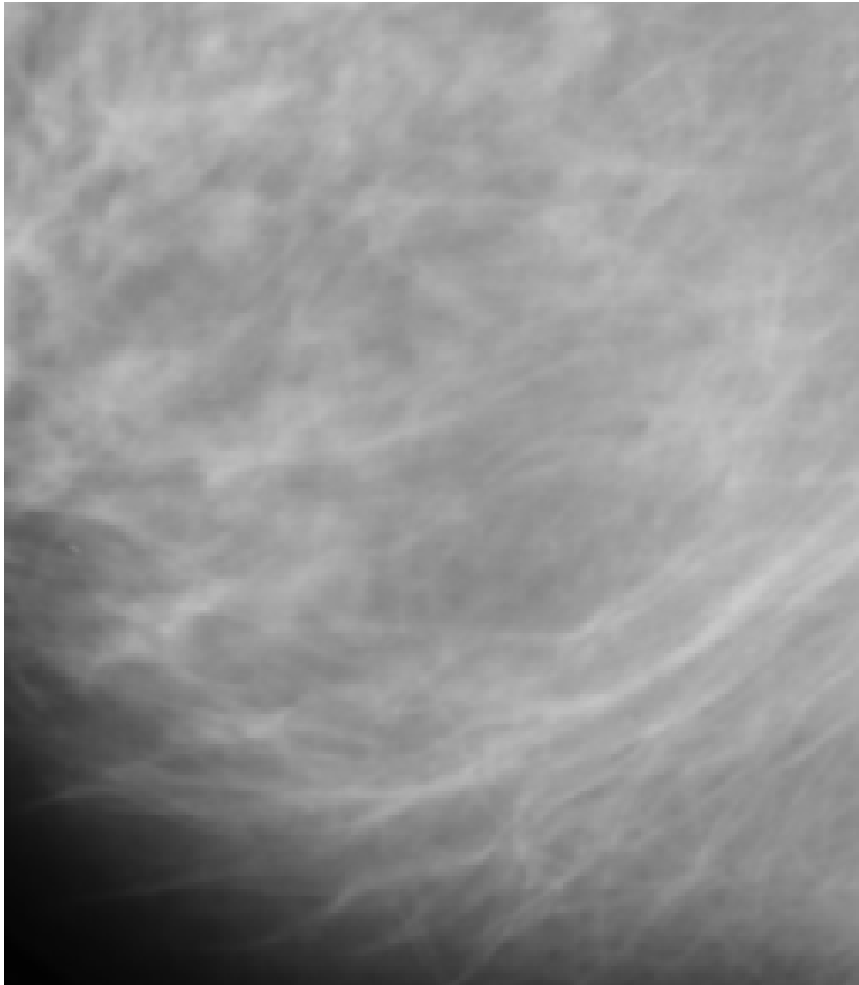


incipient mass

Normal vs. architectural distortion



Normal vs. architectural distortion





Detection of architectural distortion

1. Extract the orientation field
2. Filter and downsample the orientation field
3. Analyze orientation field using phase portraits
4. Post-process the phase portrait maps
5. Detect sites of architectural distortion

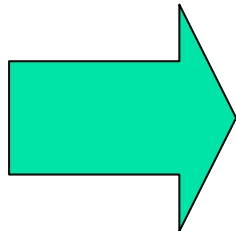


Gabor filter

$$g(x, y) = \frac{1}{2\pi\sigma_x\sigma_y} \exp\left[-\frac{1}{2}\left(\frac{x^2}{\sigma_x^2} + \frac{y^2}{\sigma_y^2}\right)\right] \cos(2\pi fx)$$

Design parameters

- line thickness τ
- elongation l
- orientation θ

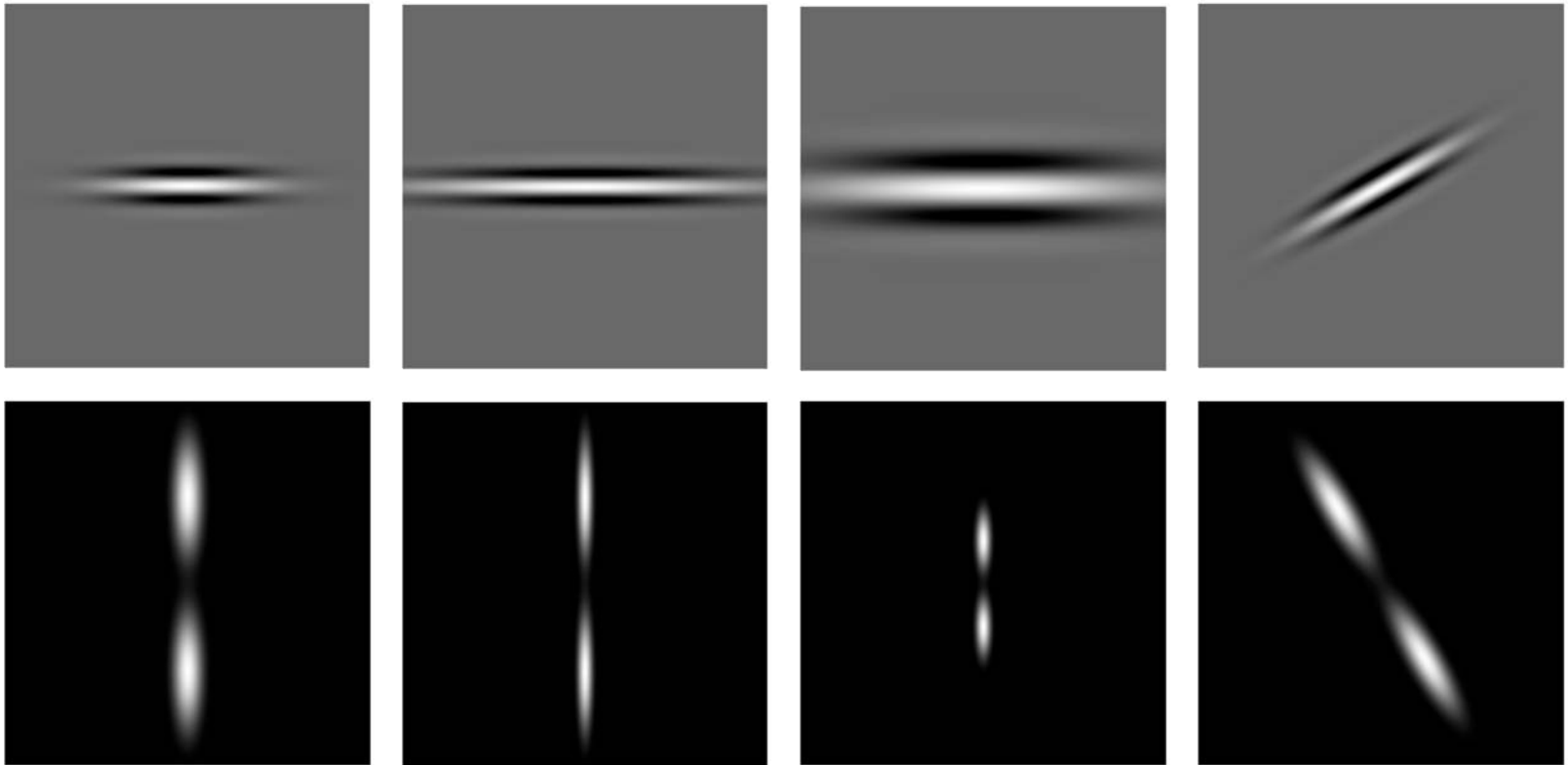


Gabor parameters

$$f = \frac{1}{\tau}; \quad \sigma_x = \frac{\tau}{2\sqrt{2\ln 2}}$$

$$\sigma_y = l\sigma_x; \quad \begin{bmatrix} x \\ y \end{bmatrix} = \begin{bmatrix} \cos\theta & -\sin\theta \\ \sin\theta & \cos\theta \end{bmatrix} \begin{bmatrix} x' \\ y' \end{bmatrix}$$

Design of Gabor filters



$$\begin{aligned}l &= l_0 \\ \tau &= \tau_0 \\ \theta &= \theta_0\end{aligned}$$

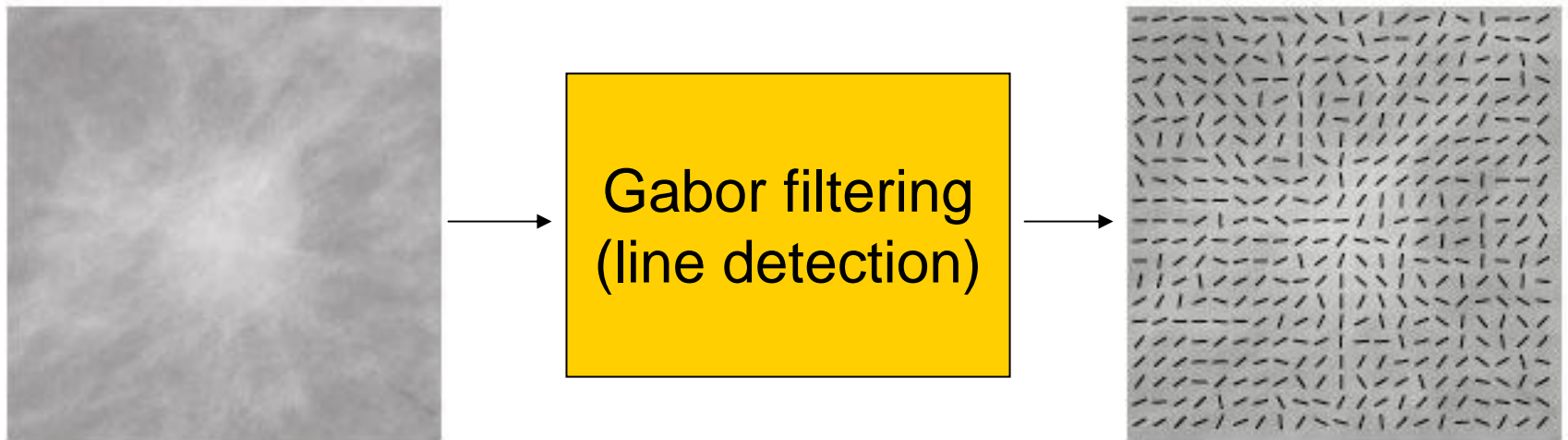
$$\begin{aligned}l &> l_0 \\ \tau &= \tau_0 \\ \theta &= \theta_0\end{aligned}$$

$$\begin{aligned}l &= l_0 \\ \tau &> \tau_0 \\ \theta &= \theta_0\end{aligned}$$

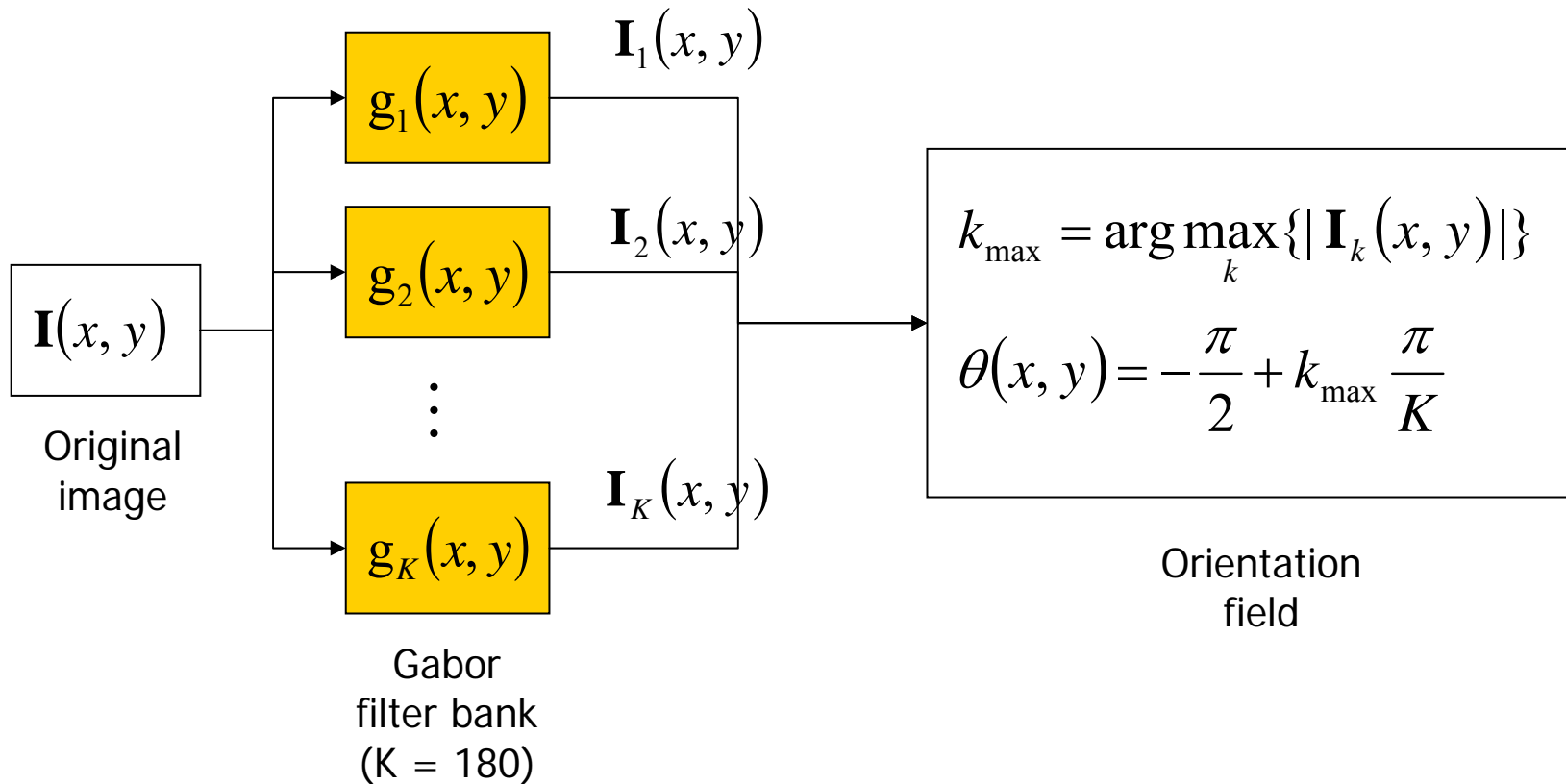
$$\begin{aligned}l &= l_0 \\ \tau &= \tau_0 \\ \theta &> \theta_0\end{aligned}$$

Extracting the orientation field

- Compute the texture orientation (angle) for each pixel



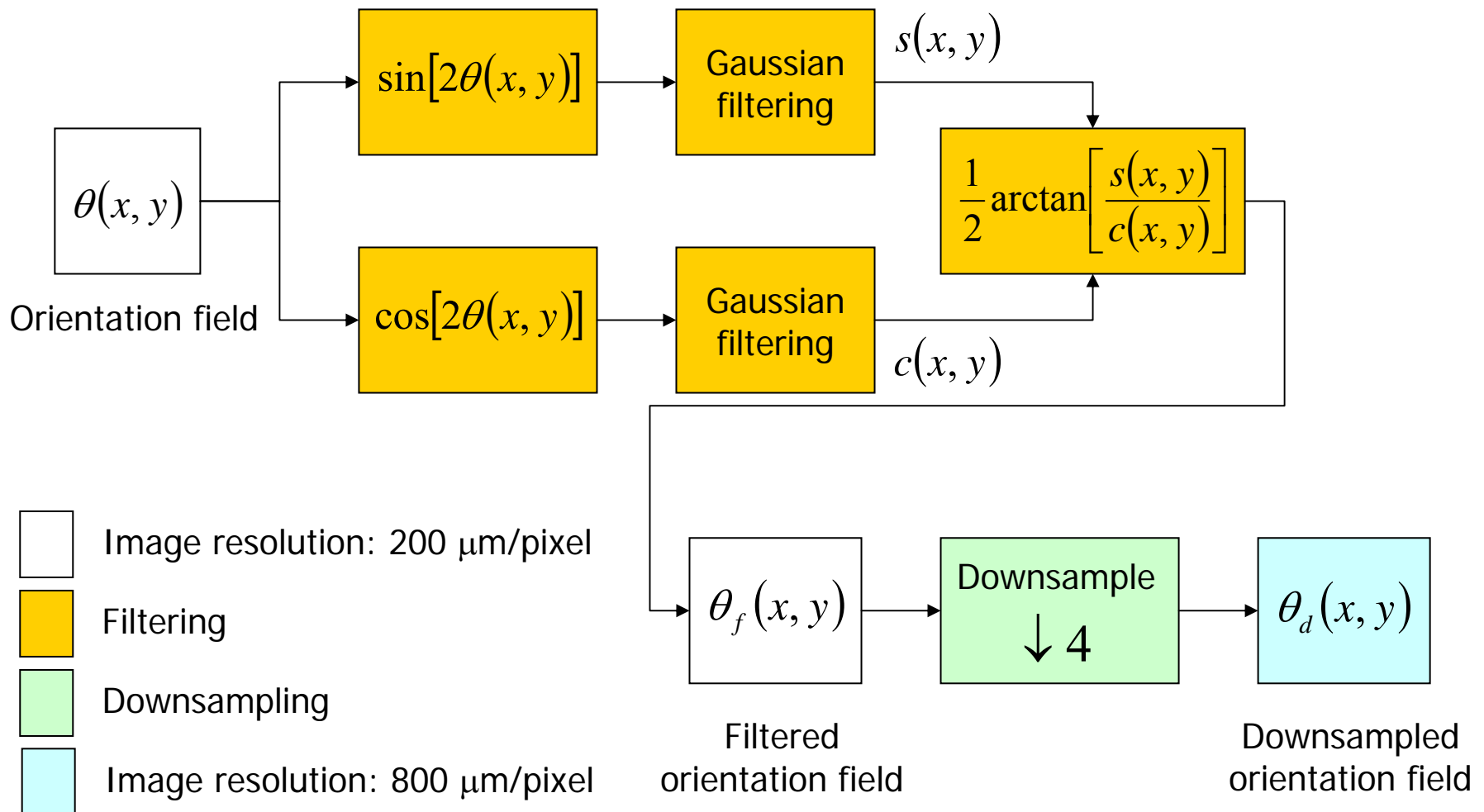
Extracting the orientation field



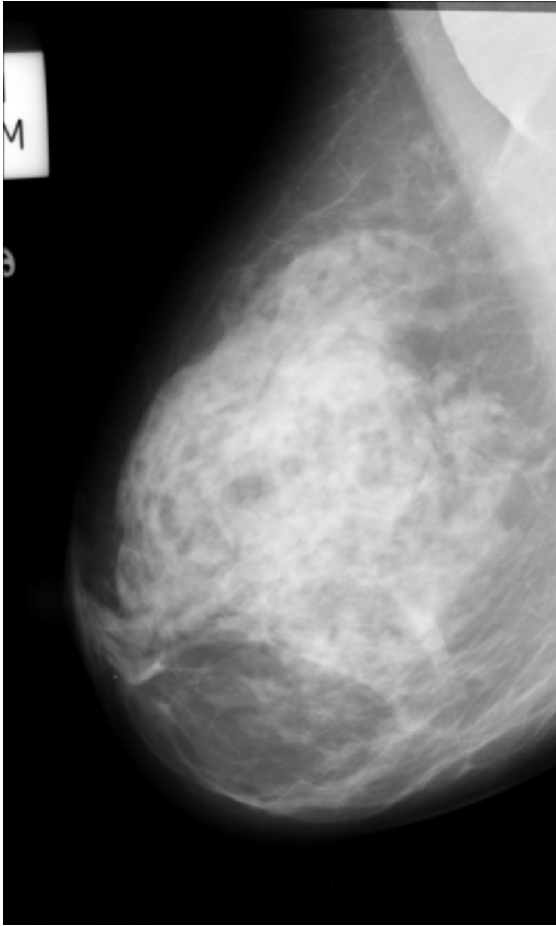
 Filtering

 Image resolution: 200 $\mu\text{m}/\text{pixel}$

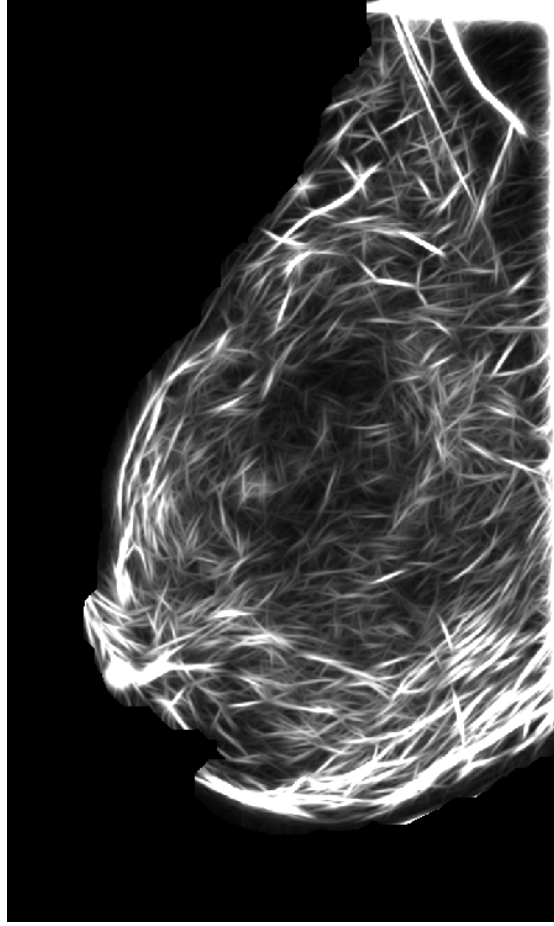
Filtering and downsampling the orientation field



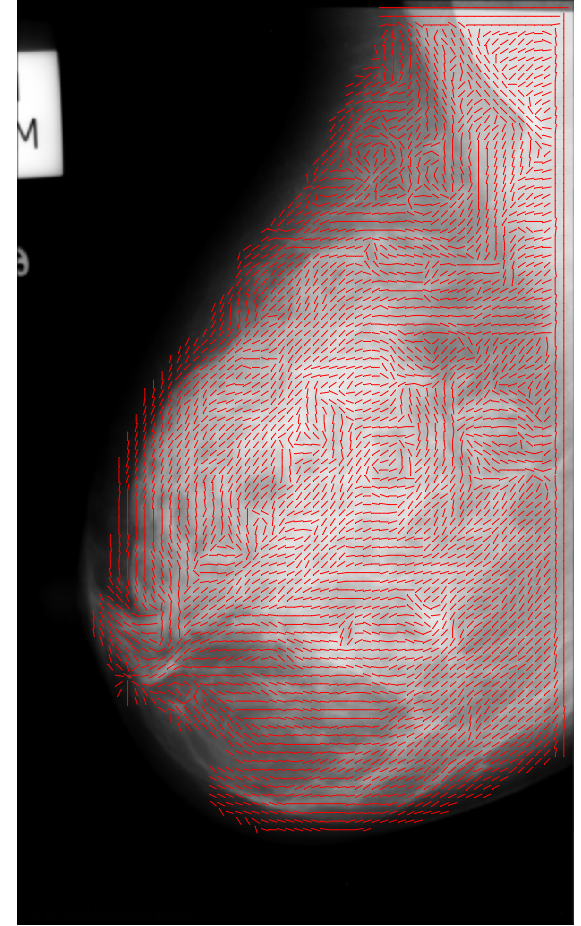
Orientation field: architectural distortion



Original image

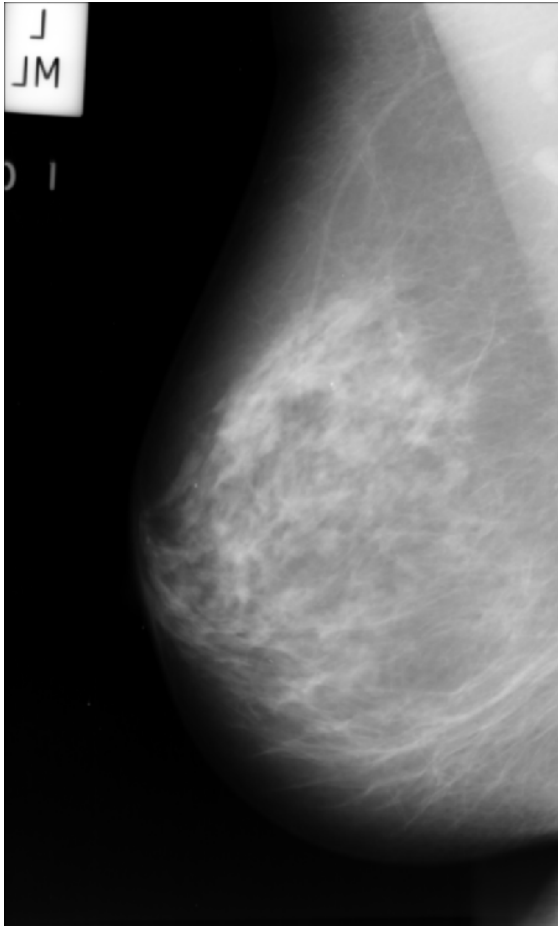


Gabor magnitude

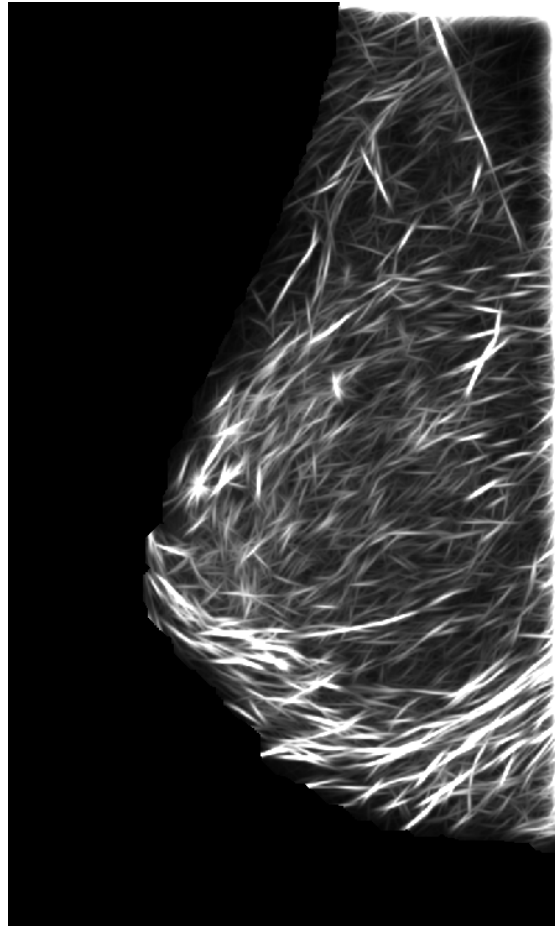


Filtered orientation field

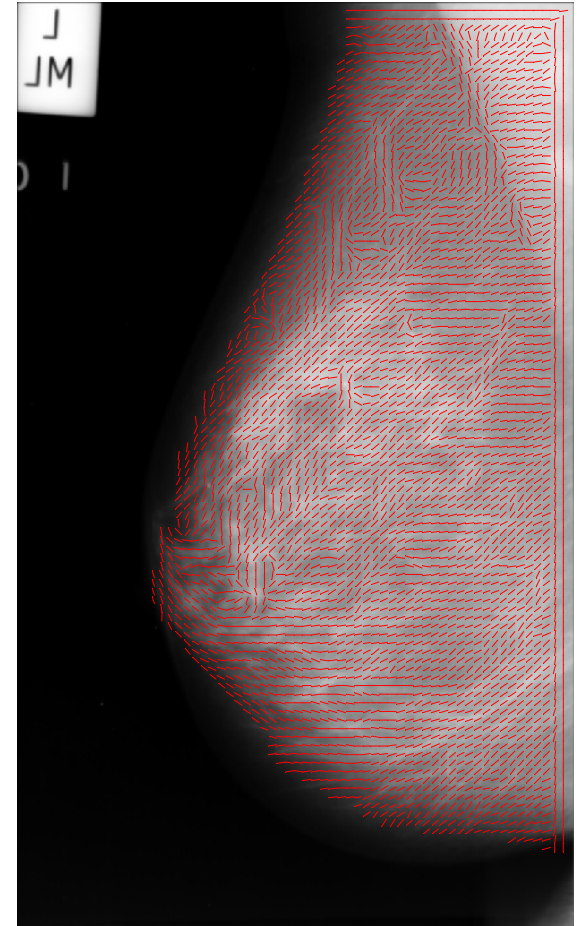
Orientation field: normal case



Original image



Gabor magnitude

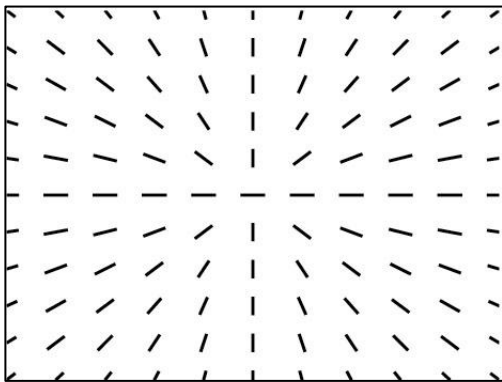


Filtered orientation field

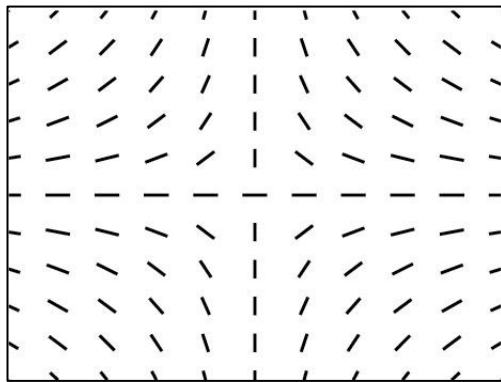


Phase portraits

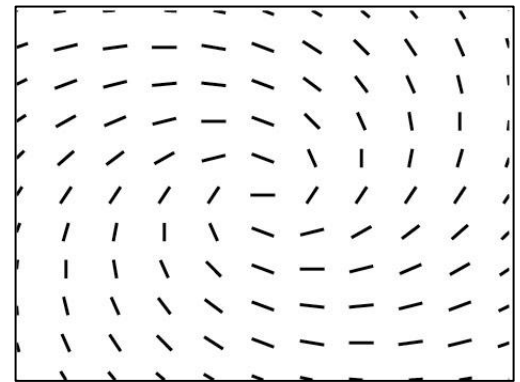
$$\vec{v}(x, y) = \begin{pmatrix} v_x \\ v_y \end{pmatrix} = \mathbf{A} \begin{pmatrix} x \\ y \end{pmatrix} + \mathbf{b}$$



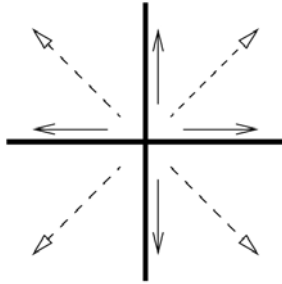
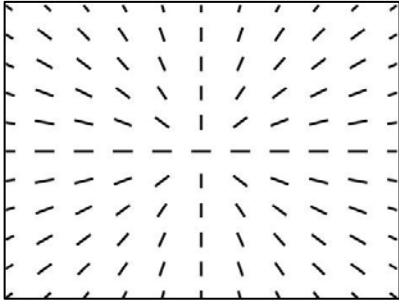
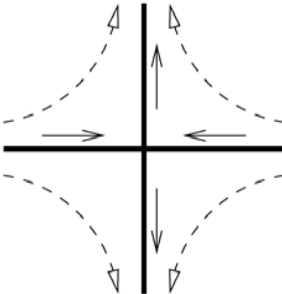
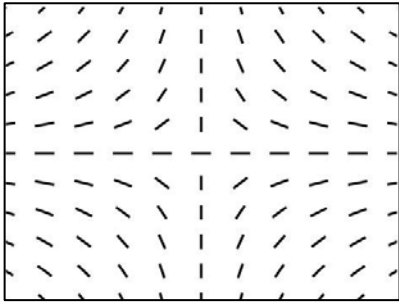
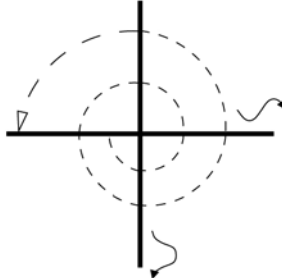
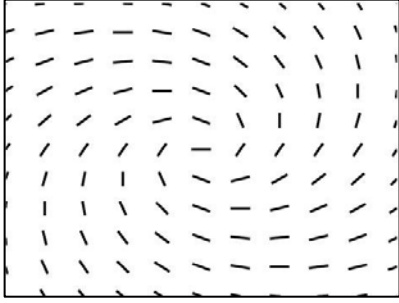
node



saddle



spiral

Phase portrait type	Eigenvalues of matrix A	Streamlines	Orientation field
Node	Real, same sign		
Saddle	Real, opposite sign		
Spiral	Complex conjugate		



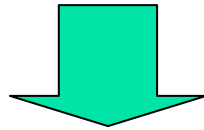
Model error

Orientation field

$$\theta(x, y)$$

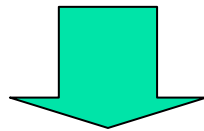
Model-generated field

$$\phi(x, y|\mathbf{A}, \mathbf{b})$$



$$\Delta(x, y) = \sin[\theta(x, y) - \phi(x, y|\mathbf{A}, \mathbf{b})]$$

Local error measure

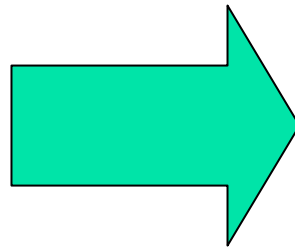
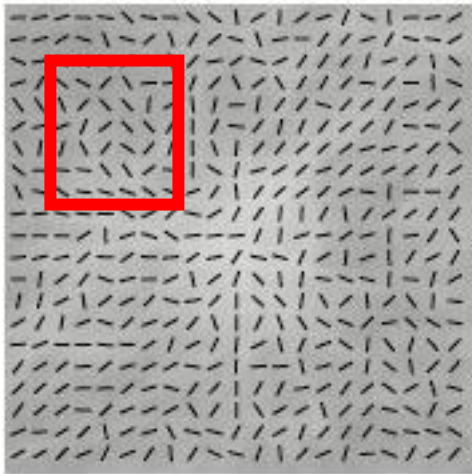


$$\varepsilon^2(\mathbf{A}, \mathbf{b}) = \sum_x \sum_y \Delta^2(x, y)$$

Sum of the squared
error measure

Texture analysis using phase portraits *(step 1 of 3)*

1. Fit phase portrait model to the moving analysis window



$$\mathbf{A} = \begin{bmatrix} 1.1 & 0.3 \\ -0.2 & 1.7 \end{bmatrix}$$

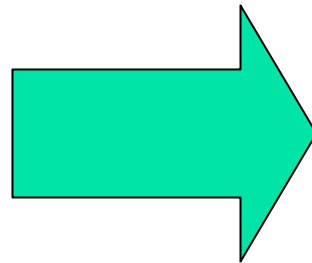
$$\mathbf{b} = \begin{bmatrix} -4.8 \\ -7.9 \end{bmatrix}$$

Texture analysis using phase portraits *(step 2 of 3)*

2. Find phase portrait type and location of fixed point

$$\mathbf{A} = \begin{bmatrix} 1.1 & 0.3 \\ -0.2 & 1.7 \end{bmatrix}$$

$$\mathbf{b} = \begin{bmatrix} -4.8 \\ -7.9 \end{bmatrix}$$

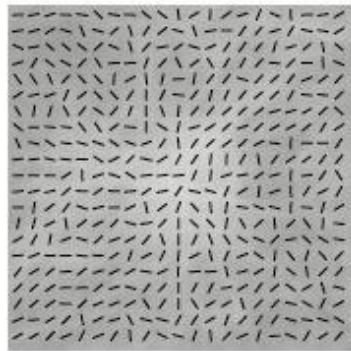


Type: node

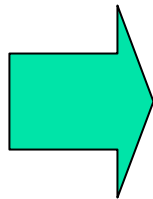
Fixed point:
 $x=3, y=5$

Texture analysis using phase portraits *(step 3 of 3)*

3. Cast a vote in the corresponding phase portrait map



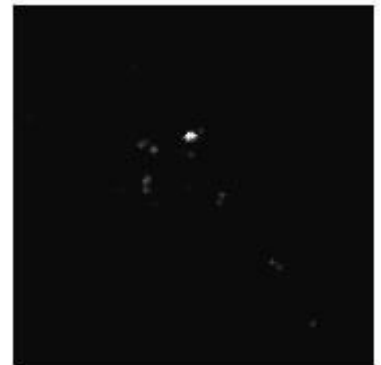
Orientation
field



Node



Saddle



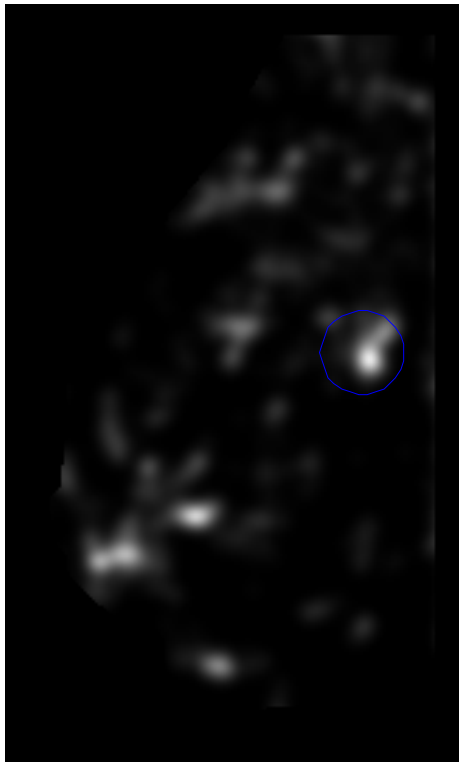
Spiral



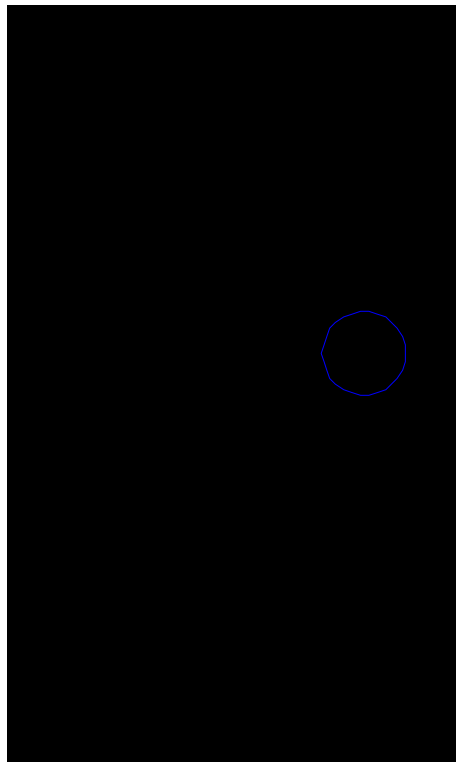
Post-processing and detection

1. Filter the node map with a Gaussian mask
2. Detect peaks in the node map larger than the other peaks within a radius of 6.4 mm (8 pixels)
3. **The peaks indicate the locations of architectural distortion**

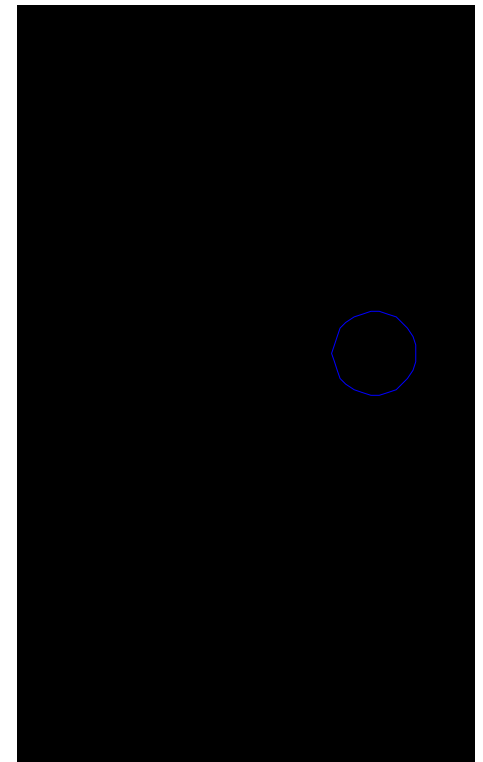
Phase portrait maps: architectural distortion case



node
[0, 1.1]

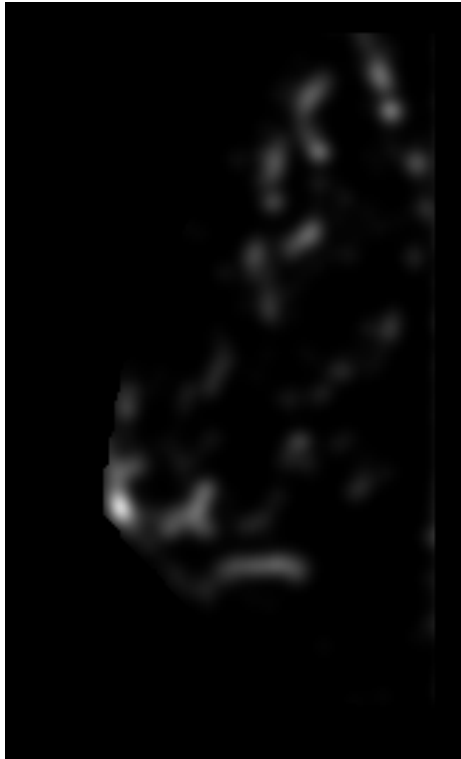


saddle
[0, 0.3×10^{-3}]

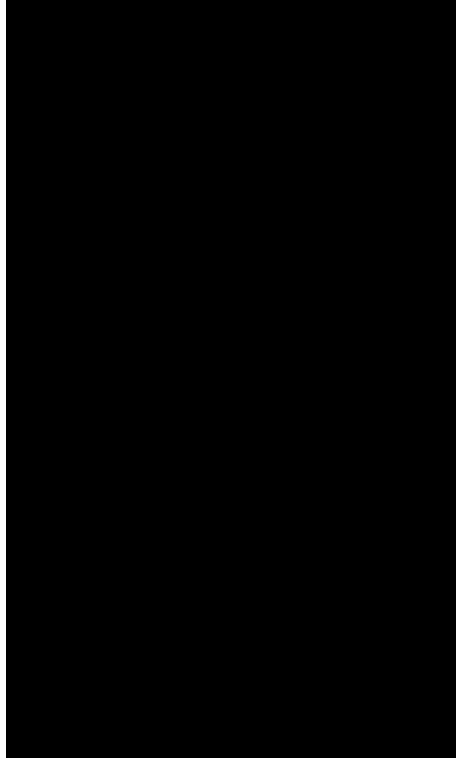


spiral
[0, 0]

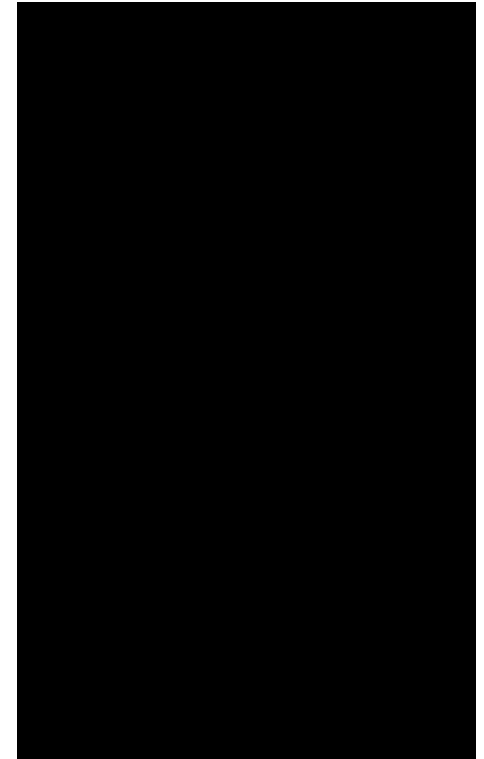
Phase portrait maps: normal case



node
[0, 0.98]

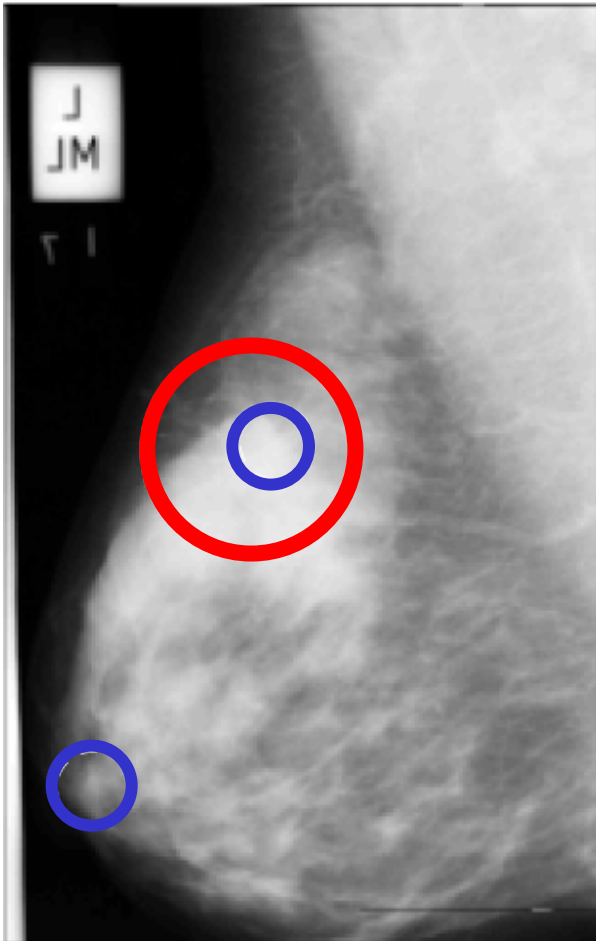


saddle
[0, 0.2×10^{-4}]



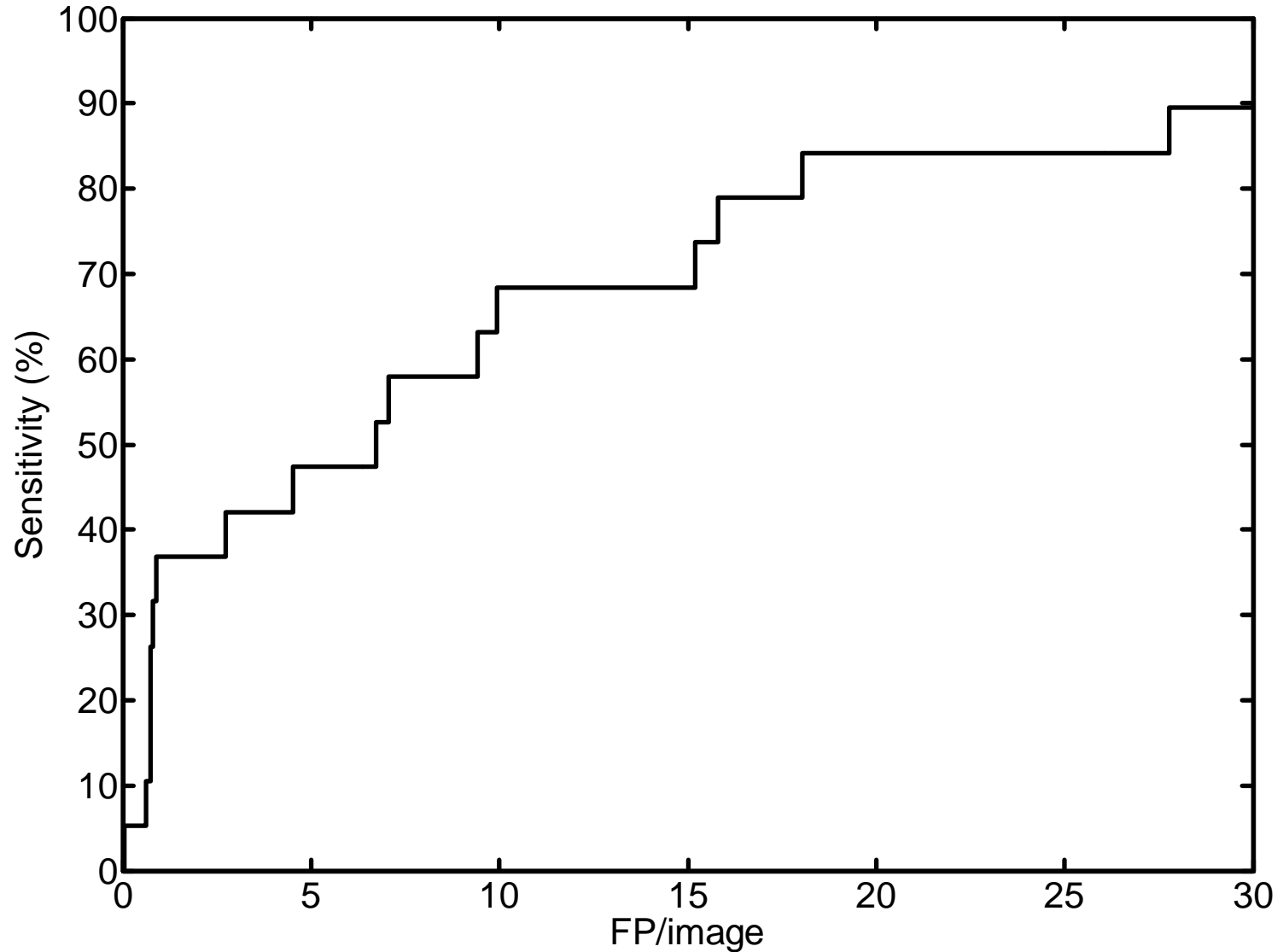
spiral
[0, 0]

Initial results of detection (2004)

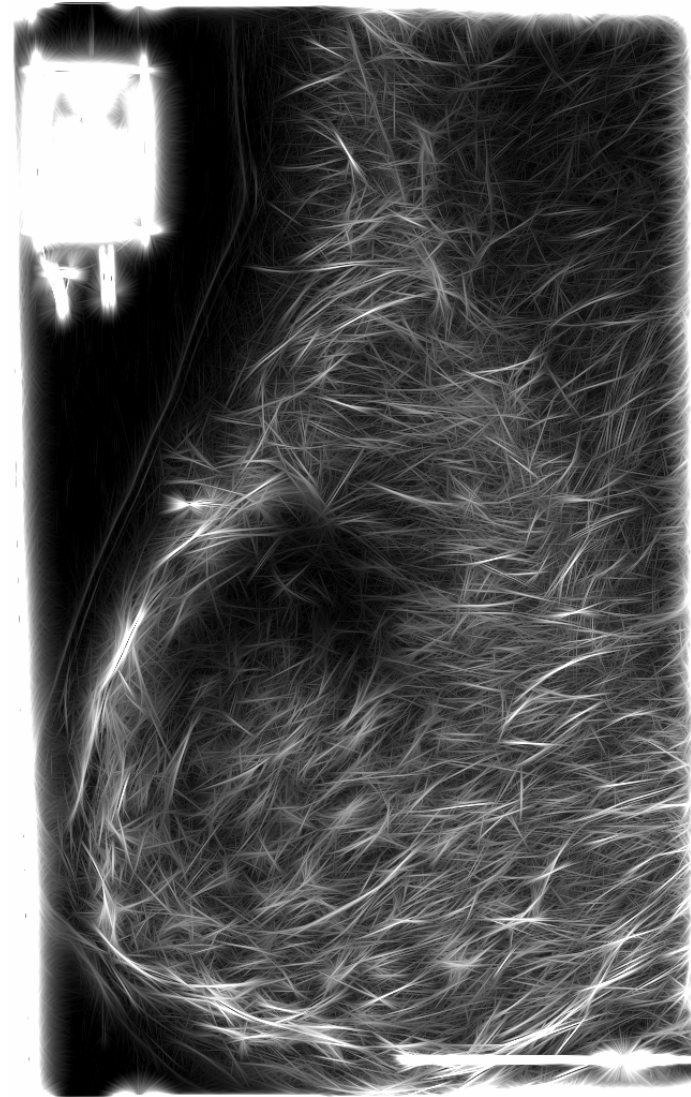


- Test dataset: 19 mammograms with architectural distortion (MIAS database)
- Sensitivity: 84%
- 18 false positives per image

FROC analysis



Reduction of false positives



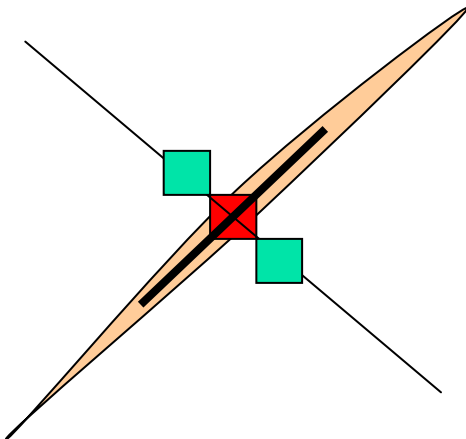


Rejection of confounding structures

- Confounding structures include
 - Edges of vessels
 - Intersections of vessels
 - Edge of the pectoral muscle
 - Edge of the fibro-glandular disk

Detection of curvilinear structures (CLS)

- Nonmaximal suppression
 - If a pixel in the magnitude image is greater than its neighbors along the direction perpendicular to the local orientation field angle, the pixel is a core CLS pixel



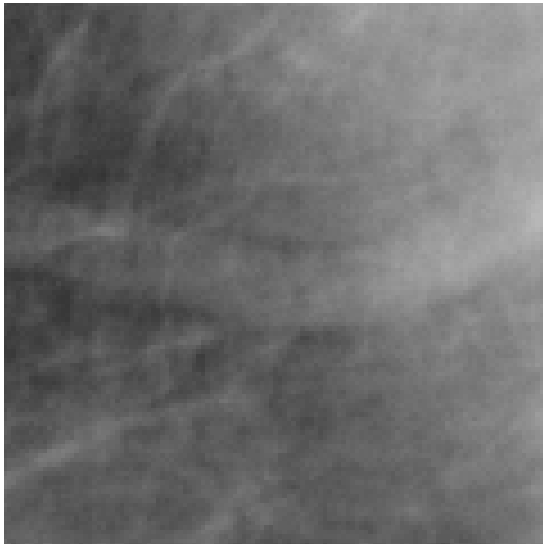
CLS

Gabor magnitude output

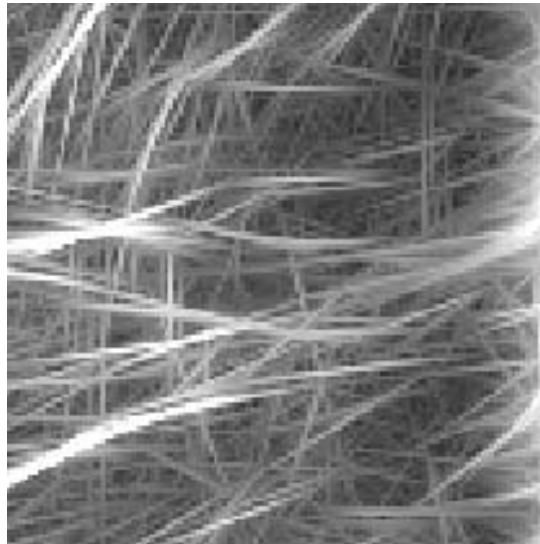
Core CLS pixel

Neighboring pixels along normal

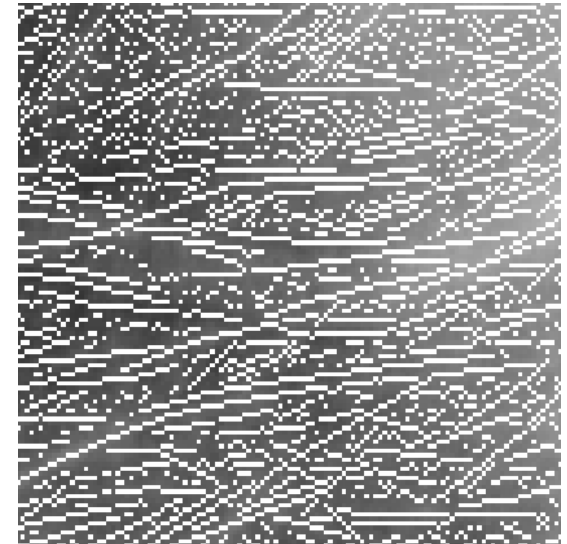
Nonmaximal suppression



ROI with a vessel



Gabor magnitude output



Output of nonmaximal suppression (NMS)



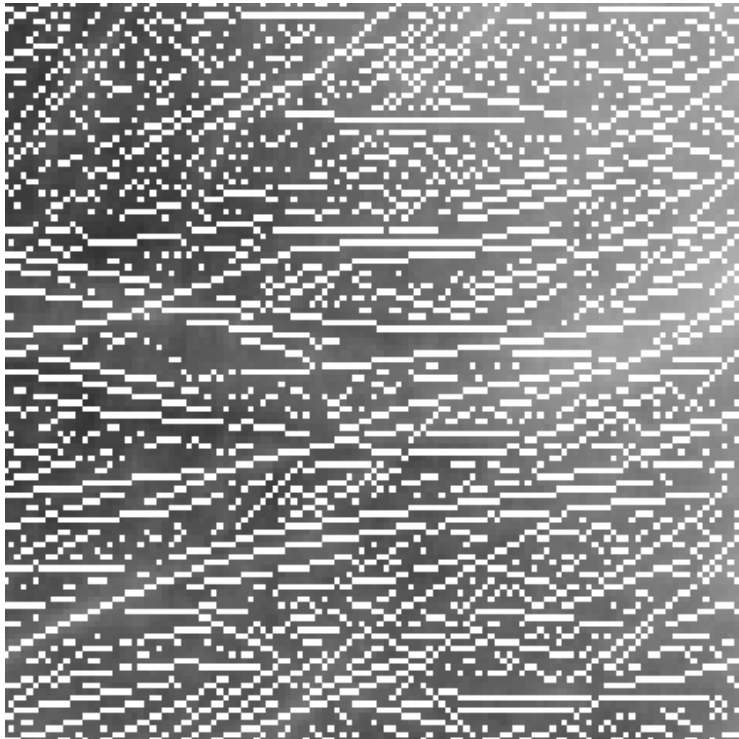
Rejection of confounding structures

- Main feature of confounding structures:

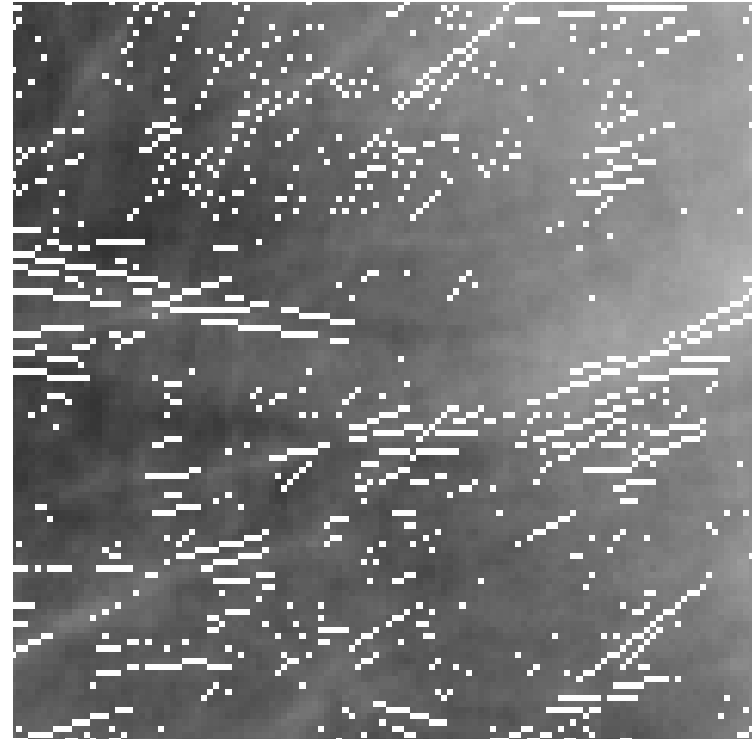
Angle from the orientation field and direction perpendicular to the gradient vector differ by less than 30 degrees

(Adaptation of a method by Karssemeijer and te Brake: IEEE TMI 1996)

Rejection of confounding CLS

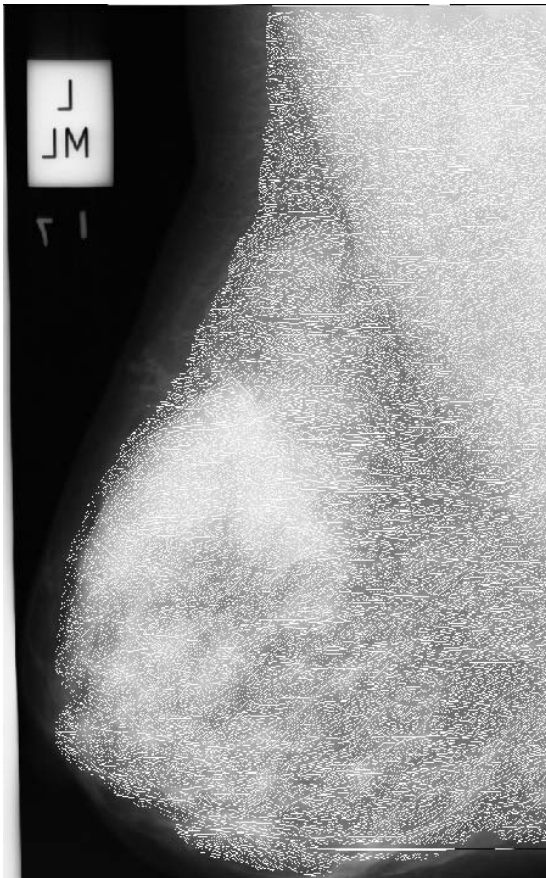


*Core CLS pixels detected
(Output of NMS)*



*CLS pixels rejected from
further analysis*

Rejection of confounding CLS



*Core CLS pixels detected
(Output of NMS)*



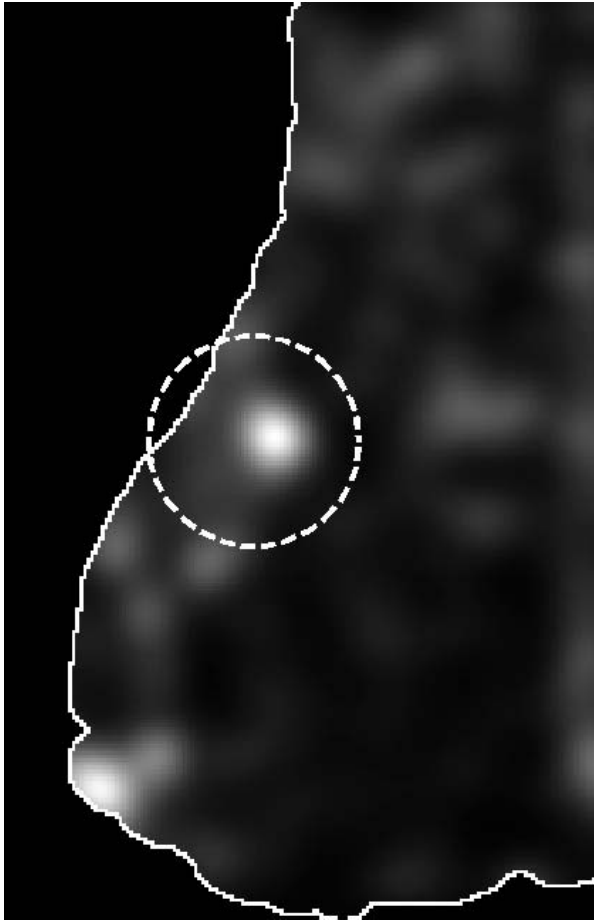
*CLS pixels rejected
from further analysis*



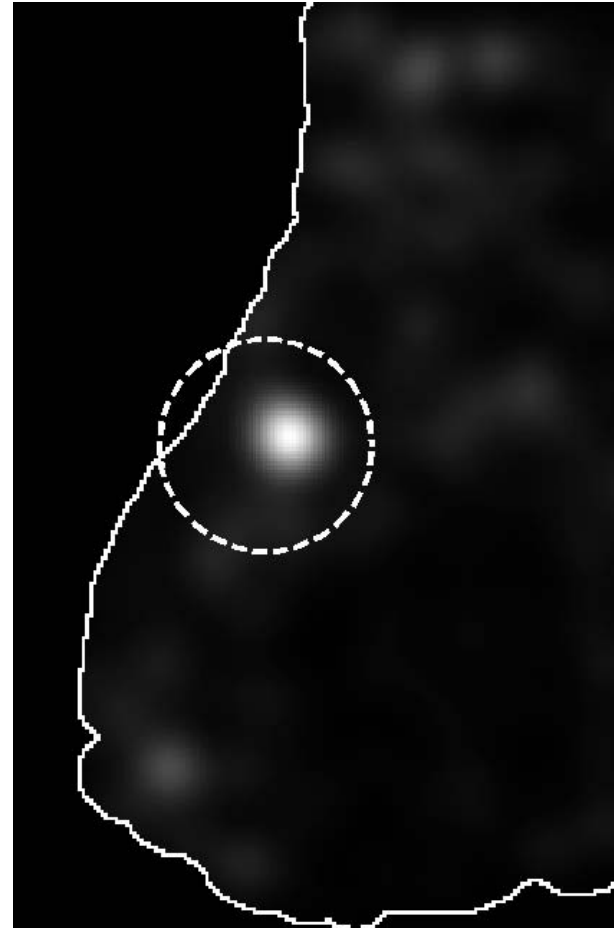
Improved phase portrait analysis

- Local error measure weighted by smoothed and downsampled map of CLS pixels
- Simulated annealing (SA) applied to obtain initial estimate of phase portrait parameters at every position of analysis window
 - Global optimization of weighted sum of squared error measure over 6-D space of \mathbf{A} and \mathbf{b}
- Parameters further refined by nonlinear least squares

Improved detection of sites of architectural distortion

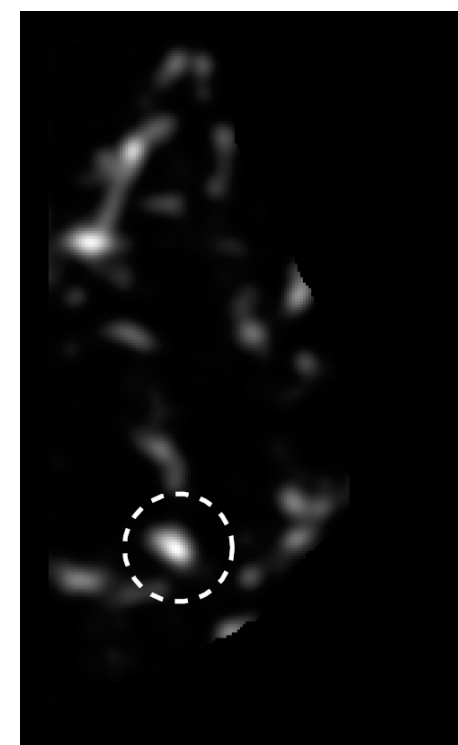
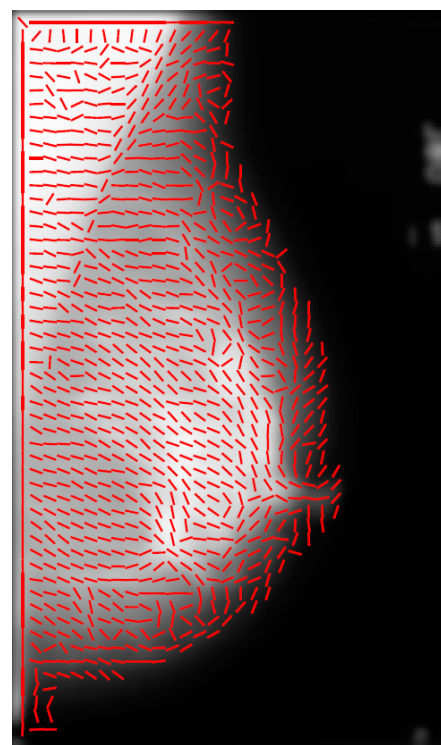
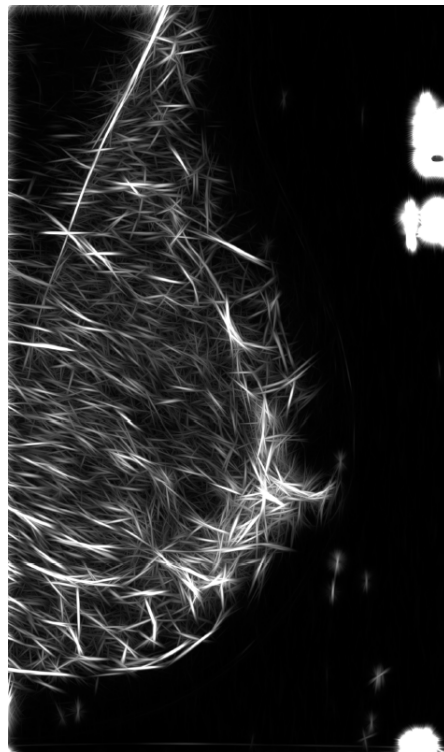
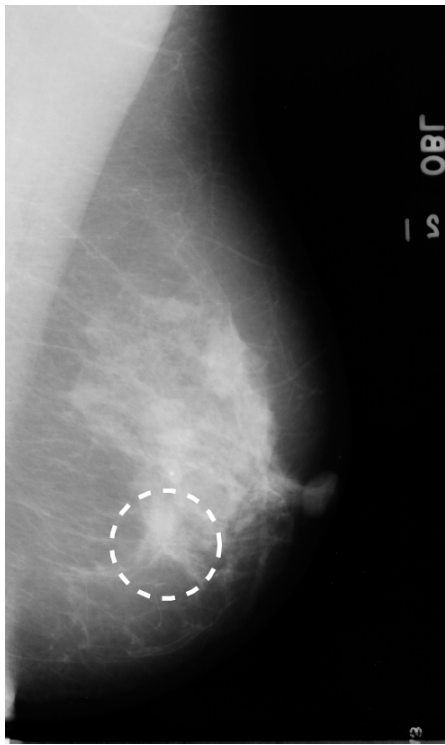


*Node map
without CLS analysis*

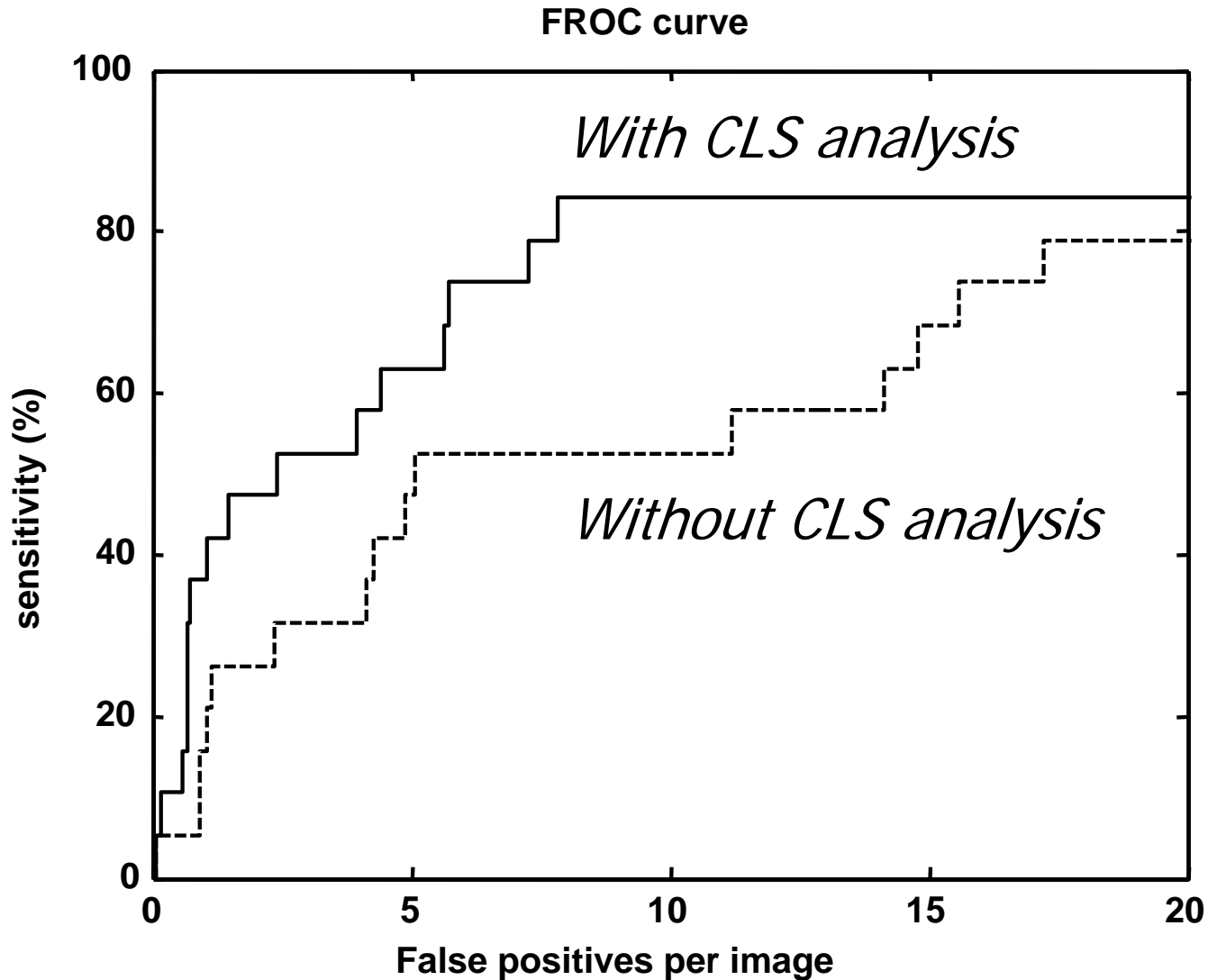


*Node map
with CLS analysis*

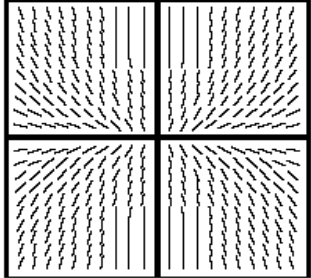
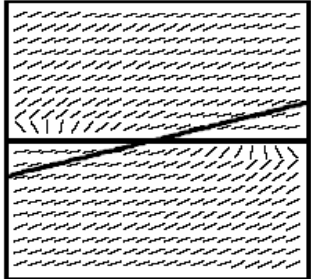
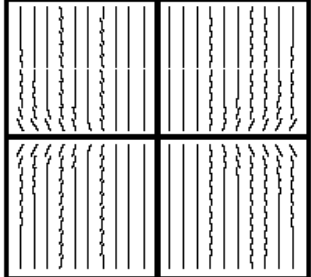
Result of detection of architectural distortion



FROC analysis (2005)



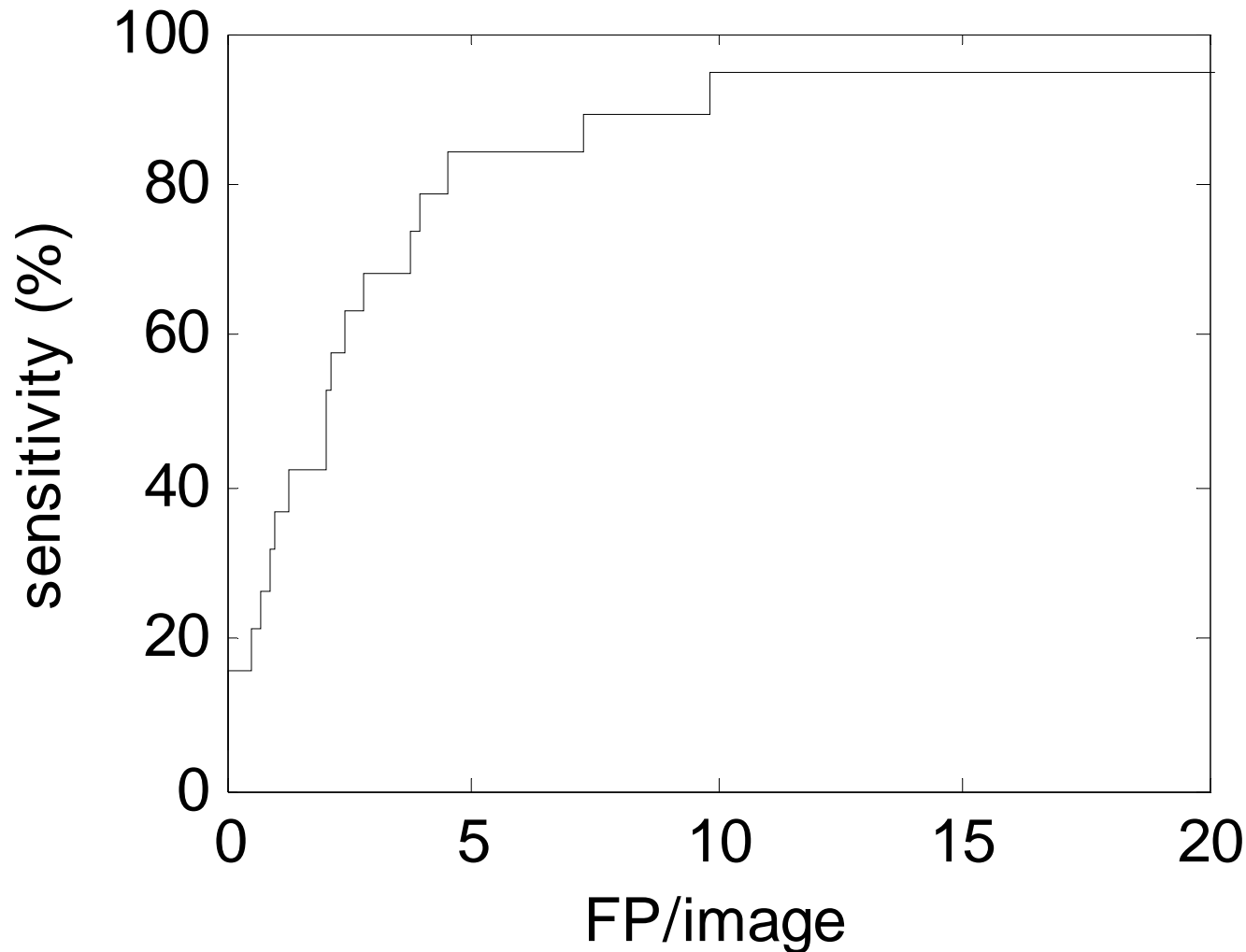
Effect of conditioning number of matrix A on the orientation field

Example	Matrix A	Eigenvalues	Angle between principal axes	Conditioning number	Orientation field
A	$\begin{bmatrix} 1 & 0 \\ 0 & 3 \end{bmatrix}$	$\lambda_1 = 1$ $\lambda_2 = 3$	90°	3	
B	$\begin{bmatrix} 1 & 7.46 \\ 0 & 3 \end{bmatrix}$	$\lambda_1 = 1$ $\lambda_2 = 3$	15°	21.85	
C	$\begin{bmatrix} 1 & 0 \\ 0 & 20 \end{bmatrix}$	$\lambda_1 = 1$ $\lambda_2 = 20$	90°	20	

Improved results (2006)

- 19 cases of architectural distortion
- 41 normal control mammograms (MIAS)
- Symmetric matrix \mathbf{A} : node and saddle only
- Conditioning number of $\mathbf{A} > 3$: reject result
- *Sensitivity: 84% at 4.5 false positives / image*
- *Sensitivity: 95% at 9.9 false positives / image*

FROC analysis with symmetric A (2006)





Conclusion and future work

- Phase portraits can be used to detect architectural distortion
- Need to reduce false positives further
- Evaluate method with a large database
- Test method with screening mammograms taken prior to mass formation:

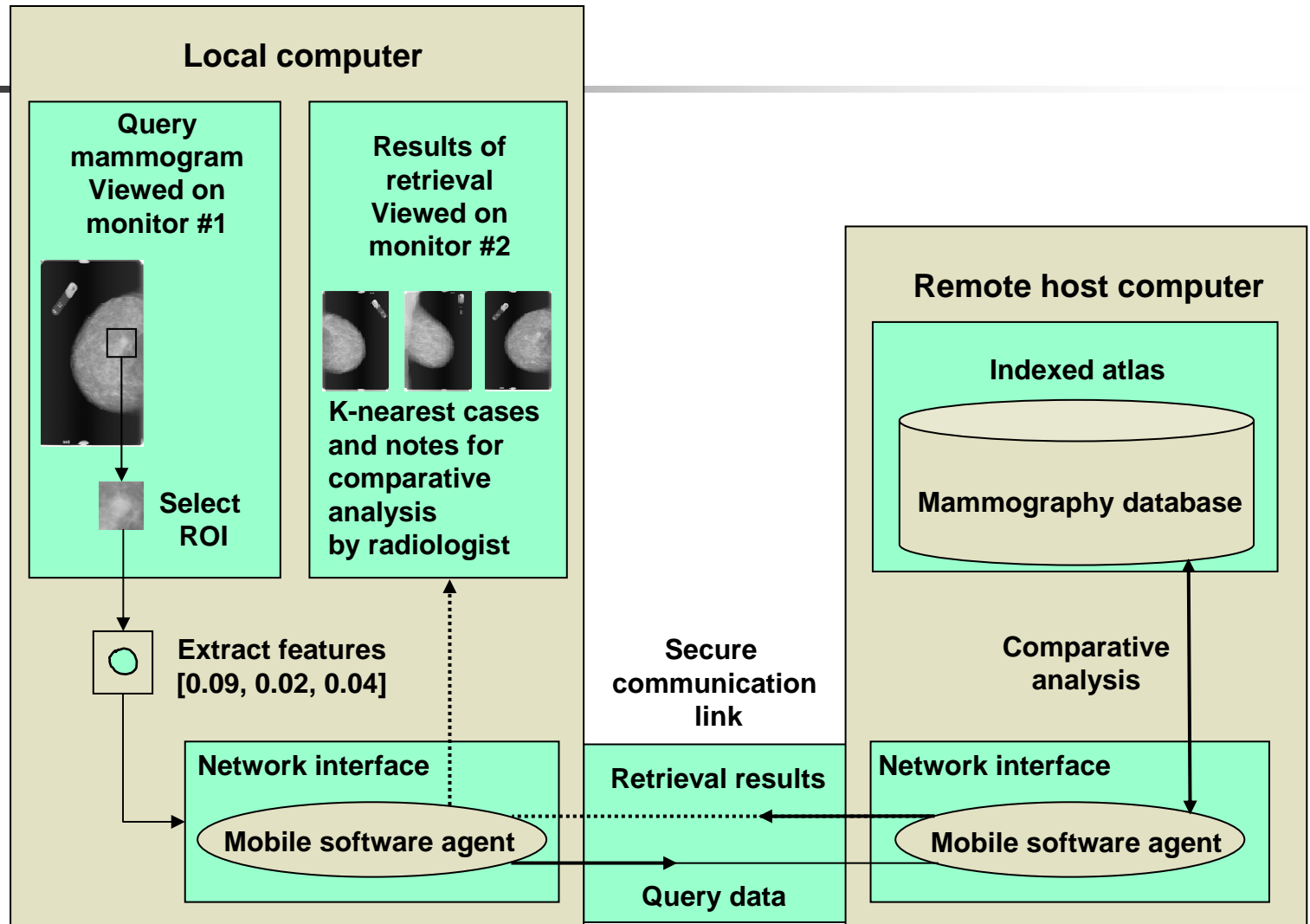
earlier detection of breast cancer



Applications of computer-aided diagnosis

- Screening program or diagnostic clinic:
 - *Consultation by radiologists*
 - *Decision support*
 - *Second opinion*
 - *Comparison with cases of known diagnosis*
- Training:
 - *Teaching, continuing medical education*
- Teleradiology, telemedicine:
 - *When local expertise is not available*

Use of the University of Calgary indexed atlas with mobile agents





Acknowledgment

- Natural Sciences and Engineering Research Council of Canada
- Alberta Heritage Foundation for Medical Research
- Canadian Breast Cancer Foundation
- Screen Test: Alberta Program for the Early Detection of Breast Cancer
- My research students, coworkers, and collaborators